

Contamination and Wettability: Rare Earth Oxides

by

Muhammad Salim

Bachelor of Science, Chemistry, Kenneth P. Deitrich School of Arts and Sciences

University of Pittsburgh, 2012

Submitted to the Graduate Faculty of the

Kenneth P. Dietrich School of Arts and Sciences in partial fulfillment

of the requirements for the degree of

Master of Science

University of Pittsburgh

2015

UNIVERSITY OF PITTSBURGH

Kenneth P. Deitrich School of Arts and Sciences
Department of Chemistry

This thesis was presented

by

Muhammad Salim

It was defended on

March 31st, 2015

and approved by

Dr. Alexander Star, Associate Professor, Department of Chemistry

Dr. Jill Millstone, Assistant Professor, Department of Chemistry

Thesis Director: Dr. Haitao Liu, Assistant Professor, Department of chemistry

Contamination and Wettability: Rare Earth Oxides

Muhammad Salim

University of Pittsburgh, 2015

Copyright © by Muhammd Salim

2015

CONTAMINATION AND WETTABILITY: RARE EARTH OXIDES

Muhammad Salim, M.S.

University of Pittsburgh, 2015

Many applications require materials that are both intrinsically hydrophobic and robust. The current technology in hydrophobic coating is limited to organic materials that are easily degraded and require lengthy processes to apply and maintain. A recent publication in *Nature Materials*, by Azimi *et al.*, suggested that rare-earth oxides (REOs) are intrinsically hydrophobic (WCA of 105°) because their electronic structure prohibits their bonding with interfacial water. This is a potentially transformative discovery because metal oxides are much more robust than organic coatings, and therefore could be used in a much wider range of applications. However, the hydrophobicity of REOs is also quite unexpected because all other metal oxides are known to be super-hydrophilic in their pristine states. In addition, given that rare earth metal ions bind water strongly in aqueous solution and bulk REO surface strongly adsorbs water, it is puzzling why REOs surface would be hydrophobic. This work will show that REO's are actually intrinsically super hydrophilic (WCA of 0°) and only exhibit hydrophobic properties upon adsorption of ambient air carbon based contaminants. Time evolution of hydrophobicity with carbon contamination is analyzed alongside different surface contamination cleaning techniques.

TABLE OF CONTENTS

LIST OF TABLES	VII
LIST OF FIGURES	VIII
LIST OF EQUATIONS	IX
1.0 INTRODUCTION	1
1.1 SURFACE ENERGY	1
1.2 WETTABILITY.....	4
1.3 ADSORPTION PROCESS OF AIRBORNE CONTAMINANTS.....	6
1.4 SURFACE CONTAMINANT INTERFERENCES WITH WETTABILITY	8
1.5 SURFACE CONTAMINATION REMOVAL.....	10
1.6 INTRODUCTION TO SURFACE CHARACTERIZATION TECHNIQUES	11
1.6.1 Atomic Force Microscopy (AFM).....	11
1.6.2 Optical Microscopy	11
1.6.3 Water Contact Angle	12
1.6.4 X-Ray Photoelectron Spectroscopy.....	13
2.0 EXPERIMENTAL METHODS	14
2.1 MATERIALS	14
2.2 SAMPLE PREPARATION METHODS	15

2.2.1	<i>Sample Transport</i>	15
2.2.2	<i>Thermal Annealing</i>	15
2.2.3	<i>UV/Ozone</i>	15
2.2.4	<i>Ar⁺ Sputtering</i>	16
2.2.5	<i>UHV Storage</i>	16
2.2.6	<i>Solvent Cleaning</i>	16
2.3	CHARACTERIZATION METHODOLOGY	18
2.3.1	<i>XPS Methodology</i>	18
2.3.2	<i>WCA Methodology</i>	20
2.3.3	<i>Optical Microscopy Methodology</i>	20
2.3.4	<i>Atomic Force Microscopy Methodology</i>	21
3.0	WETTABILITY AND RARE EARTH OXIDES	22
4.0	RESULTS AND DISCUSSION	25
4.1	WETTABILITY OF GADOLINIUM AND DYSPROSIUM (REOs) FOILS	25
4.2	WETTABILITY OF CERIUM OXIDE THIN FILM.....	28
4.3	SURFACE DEFECT ANALYSIS (XPS)	38
4.4	PEAK RATIOS TO QUANTIFY CE ⁴⁺ :CE ³⁺ RATIO.....	47
5.0	CONCLUSIONS AND FUTURE DIRECTIONS	51
	REFERENCES	53

LIST OF TABLES

Table 1. Surface Free Energies of Particular Solids and Liquids. ^{3,4}	3
Table 2. WCA and Surface Carbon Content of CeO ₂ Samples	36
Table 3. Relative Composition of Single Peaks and Correlation Factors	49
Table 4. Ce ⁴⁺ and Ce ³⁺ Peak Ratios After Cleaning and Aging	49

LIST OF FIGURES

Figure 1. Pictorial Diagram of Surface Tension and Surface Energy.....	2
Figure 2. Contact Angle.....	5
Figure 3. Fruit Basket Model.....	7
Figure 4. Schematic of the orientation of water molecules and the associated wetting	23
Figure 5. Time Evolution of Air Exposed REOs.....	26
Figure 6. XPS Spectra of as-received and treated CeO ₂ thin films	33
Figure 7. WCA of Treated CeO ₂ films	34
Figure 8. WCA of CeO ₂ thin films annealed at 500°C.....	35
Figure 9. Surface Morphology Characterization of annealed CeO ₂ Thin Films.....	36
Figure 10. Ce3d _{3/2,5/2} XPS Spectra of Ce(IV) oxide and Ce(III) oxide	39
Figure 11. Cerium XPS spectra of as-received, untreated, CeO ₂ thin film	40
Figure 12. Cerium XPS spectra after 500°C annealing for 1hr.....	41
Figure 13. Cerium XPS spectra of 500°C annealed sample exposed to ambient air for 2 weeks. 42	
Figure 14. Cerium XPS spectra after UV/Ozone treatment for 20 minutes	43
Figure 15. Cerium XPS spectra after Solvent Washing.....	44
Figure 16. Cerium Oxide spectra comparison after Ar ⁺ sputtering at 4000eV.....	45
Figure 17. Cerium Oxide spectra comparison after Ar ⁺ sputtering at 500eV.....	46

LIST OF EQUATIONS

Equation 1 Contact Angle Relation.....	5
Equation 2 Relation of Correlation Factor to Total Peak Integration.....	47

1.0 INTRODUCTION

1.1 SURFACE ENERGY

Surface energy is defined in terms of the free energy change when a solid is separated into two pieces at a large distance. This separation disrupts energetically favorable bonds between the once connected atoms within the solid, essentially increasing the free energy in these now exposed regions.^{1,2} Consider atoms in the bulk and on the surface of a solid lattice. The atoms contained within the bulk lattice have neighboring atoms which form energetically favorable bonding and interactions. This reduces the overall internal energy of the bulk system. The process of atoms and molecules maximizing favorable interactions is what ultimately determines the results of surface energy measurements and observable phenomena. Since there are more of these interactions in the bulk of a material, the summation of these net favorable attractive forces ultimately results in a net inward force. This contracts the substrate equally inward from all directions, up to the point where it is balanced out by repulsive forces within, much like a droplet of water.^{1,2} This same notion also applies for non-deformable surfaces, such as solids.

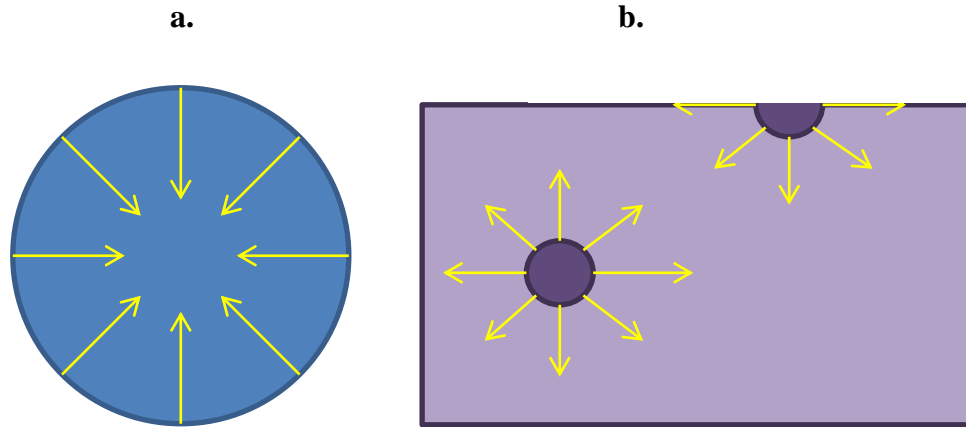


Figure 1. Pictorial Diagram of Surface Tension and Surface Energy| a, Net attractive forces on a water droplet, forming a sphere. **b,** Comparison of net attractive forces of atoms on the surface or in the bulk of a solid.

This summation of net attractive forces is what causes water droplets to produce spherical shapes in air, and what also gives them the ability to maintain their shape when in contact with a solid surface. It is also important to consider the net interactions of surface atoms on the solid. Unlike within the bulk, there is a limitation on the number of nearby similar atoms, reducing the number of favorable interactions. Because of this, surface atoms will have to be in a higher energetic state than the atoms contained within the bulk. Therefore, the degree in which they are able to reduce their free energy by bonding/interacting with lattice atoms is less than the bulk is able to, due to their position on the surface.^{1,2} This results in excess energy on the surface of the substrate, hence the term ‘surface free energy.’

The progressive reduction of surface free energy is the driving force of these naturally occurring processes, like a water droplet forming a sphere, which brings the system to a lower energetic state. Therefore, the reduction of surface energy is not just limited to like-molecules, but can be applied to molecules which are able to produce a net reduction in the surface free

energy. Any net favorable interactions from surrounding molecules are able to reduce surface energy via adsorption or chemical bonding.³ Distance and relative concentration of the molecules should also be taken into consideration, as these processes are considered a probability.³ These factors contribute to the molecules orienting themselves as particular ‘layers’ on the surface of the substrate, gradually reducing the surface energy of substrates in the most energetically favorable way.³ This is why the topic of contamination and contamination removal becomes an issue. Surface energy reduction is a spontaneous process that begins instantaneously on a prepared pristine surface—by the adsorption of molecules from the medium surrounding the substrate.

For samples left in ambient air conditions, these contamination layers will adsorb over time during exposure. These contamination layers owe their origin to the steady reduction of surface energy—from high energy to low energy, eventually equilibrating with the surrounding atmosphere. The surface energies listed in **Table 1** represent the generic surface energies of particular subsets of molecules.^{3,4}

Table 1. Surface Free Energies of Particular Solids and Liquids. ^{3,4}

Surface	Surface Free Energy (mJ/m²)
Liquid Air	20
Hexane	18
Decane	24
Dodecane	25
Epoxides	50
Formamide	58
Water	73
Metal Oxides	200-500
Metals	1000-5000

Different solvents and molecules have different surface energies. As do the particular molecules in the surrounding medium. Identical samples prepared simultaneously with identical parameters, but stored in different ambient air conditions, will have the same generic hierarchical layering of contaminants, but the exact chemistry composition of the adsorbed molecules is dependent upon the concentrations and identity of molecules in the surrounding storage atmosphere, as well as the identity of the substrate.^{3,5} This results in a different composition of the surface energy reduction layers on each sample.^{6,7}

1.2 WETTABILITY

Wettability measurements provide a rapid method for analyzing the outermost surface energy of a material. In order to understand wettability measurements, one must understand the forces which impact such analysis. Given a drop of water deposited on an ideal homogeneous solid, it will contact the substrate in a disc of radius ℓ . At the edge of the droplet, where outermost surface of the solid and liquid are interacting with one another; there is an observable angle θ . The value of this contact angle was first discussed by Young.⁸ Each interface draws a contact line so as to minimize the corresponding surface area. This yields a relation attributed to Young, where the equilibrium contact angle θ is determined by the liquid-solid interface energy γ_{SL} , the solid-vapor interface energy γ_{SV} , and the liquid-vapor interface energy γ_{LV} , via equation (1) (**Figure 2**).^{1,2,8}

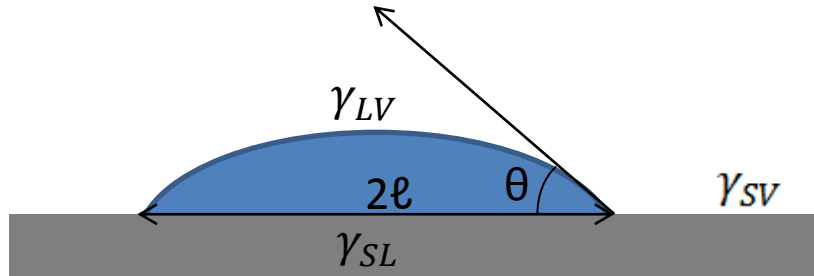


Figure 2. Contact Angle | Schematic of the forces taking place on a droplet of water residing on a surface, which play a role in determining the resulting contact angle θ .

$$\cos(\theta) = \frac{\gamma_{SV} - \gamma_{SL}}{\gamma_{LV}} \quad (1)$$

Liquids with a strong attraction to the surface of a material will expand over the material, increasing the radius of the droplet and the number of liquid-solid interactions. This type of attraction results in a lower water contact angle (WCA) ($< 90^\circ$)—indicative of a hydrophilic surface. The solid is therefore lowering its surface energy by being wetted.^{1,5,8} Alternatively, if the liquid molecules are more strongly attracted to one another than the surface of the substrate, the liquid beads-up and minimizes contact with the surface, or low wetting. This produces a high WCA ($>90^\circ$)—indicative of a hydrophobic surface. The lower the contact angle on a surface, the stronger the liquid-solid interactions, and vice versa.

1.3 ADSORPTION PROCESS OF AIRBORNE CONTAMINANTS

There are several factors to take into consideration when discussing the process of molecular adsorption on sample surfaces. After physical contact between an adsorbing molecule and surface is made, the primary interactions which take place are van der Waals and electrostatic attractive forces. Once a molecule is adsorbed onto a surface, it cannot be assumed that it will remain there until the surface is manually cleaned.⁹ There is a probability of adsorption/desorption (addition/removal) for any molecule on a surface. This is referred to as the sticking probability of the molecule, or how easily and how strongly it is adsorbed to the surface.^{9,10,11} This value not only depends on the surrounding molecules composition and their concentrations, but also the exact surface chemistry of the particular substrate. For example, if a high surface energy substrate were to be stored in ambient air conditions in a laboratory, organic compounds with the higher vapor pressures would adsorb onto the surface first and at a high rate. Lower vapor pressure compounds would also adsorb, but at a much lower rate.^{9,11,12} Each of these processes is dependent on relative favorable interactions of the molecules with the surface and surrounding air. As total air exposure time increases, the higher vapor pressure molecules are slowly replaced by organic compounds with much larger affinities for the surface and lower vapor pressures.^{9,12} This adsorption, desorption, and/or replacement process is gradually reducing the surface energy of the substrate. At first, the substrate acquires the fastest and smallest molecules to its surface at a much higher rate than the lower vapor pressure compounds,

reducing the surface energy. However, as the number of vacant sites for adsorption reduces over time, the larger molecules with a much higher affinity for the surface offer a much more effective answer to this surface reduction process.^{9,12,13} They effectively replace the higher vapor pressure organic molecules. The particular kinetics of this process have been studied and reported for contaminants on a Si wafer.¹² This replacement phenomenon is referred to as the *fruit basket model*. A pictorial example of this process is shown in Figure 3.^{9,12}

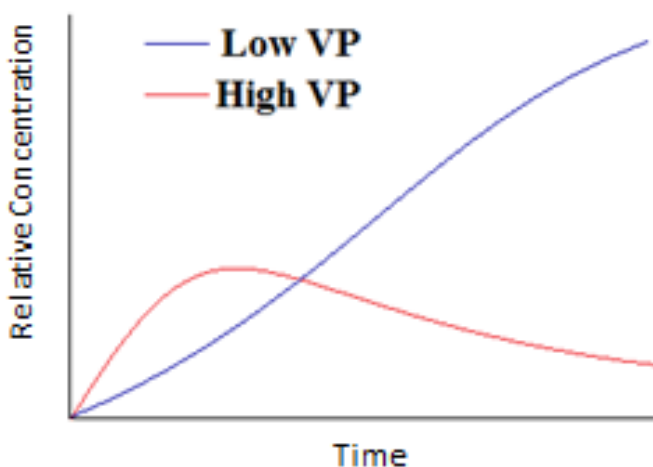


Figure 3. Fruit Basket Model | The time evolution of general relative concentrations of two carbon-based contaminants, each of differing vapor pressures (VP), residing on a sample.⁹

To analyze and observe such phenomena, like the fruit basket model, techniques such as secondary ion mass spectroscopy (SIMS) or thermal desorption coupled with mass spectroscopy (TD-MS) can be used.¹⁴ X-Ray Photoelectron Spectroscopy (XPS) would be another valid method to quantify the contamination level via carbon peak analysis, but this would not give the degree of molecular data that would be acquired by SIMS or TD-MS. If the question of contamination is not molecular composition, but the magnitude of the surface energy on the

sample, alternative surface analysis techniques, such as WCA, can be implemented. WCA provides immediate results with minimal sample preparation.

1.4 SURFACE CONTAMINANT INTERFERENCES WITH WETTABILITY

Complete wetting with water occurs for solids of high surface energy, such as transition metals, glass, or noble metals. Previous studies have shown that rare earth oxides (REOs) have high energy surfaces, such as cerium oxide (CeO_2). Multiple experimental measurements and theoretical calculations have reported its surface energy to be around 1 J/cm^2 .¹⁵⁻¹⁷ This value is characteristic of a high energy (i.e., hydrophilic) surface. In comparison, the surface energy of graphite is about 20 times smaller (ca. 55 mJ/cm^2).¹⁸ A hydrophilic surface is expected for CeO_2 , given the high melting point of REOs, which is indicative of high lattice energies of in these materials.

Glass, for example, is wetted by water when its surface is pristine and fresh right as it comes out of the factory, and often only shows partial wetting later on. However, cleaning the glass with a strong acid allows it to recover its hydrophilicity with water. The strong acid is able to remove the contamination layers on its surface. Therefore, the surface recovers its pristine hydrophilic properties upon the removal of contaminants from the outer layers on the surface of the glass.

Any surface-sensitive analysis technique, such as WCA provides information on the outermost molecular layers of a substrate. If WCA were to be performed on a contaminated substrate, even if only a monolayer is adsorbed, the measurements would be affected by the

contamination layer adsorbed to the sample in question, not just the substrate surface underneath.¹⁴ The end result of which would make a surface, which may actually be hydrophilic, appear to be hydrophobic because of the adsorbed carbon based contaminants. However, it is important to note that the eventual composition of the contamination layer is dependent on the interaction of the contamination molecules and the substrate surfaces. Contamination and wettability will vary in different storage locations and between different substrates.^{9-12,14}

On the broad scale of contamination adsorption, control and cleanliness are the primary concerns. This is especially the case in the semiconductor or medical equipment industries—where reliability, performance, and cleanliness are all significantly impacted by even extremely low levels of airborne organic contamination. The term contamination has various meanings, but this particular focus concerns the cleanliness of surfaces at the atomic scale from airborne organic materials. Organic compounds commonly found in the laboratory are generally hydrophobic in nature (ex. common solvents or vacuum-pump oil vapor). If adsorbed to a surface they will affect measurements on the outermost surface chemistry of the substrate, increasing the hydrophobic nature of the surface. Airborne hydrocarbons are known to adsorb onto a wide range of surfaces (e.g., Au, TiO₂, SiO₂, and graphene), resulting in a universal increase of their water contact angle (WCA).¹⁹ The magnitude and kinetics of this contamination-induced wettability change is sensitive to the chemical nature of the substrate and the local environment. *e.g.*, the same air exposure may result in a much smaller increase of WCA on one surface than another (ex. NiO vs TiO₂).

When airborne contaminants physically contact a solid surface, the forces between them are primarily attractive in nature. This results in the adhesion of the particle to the surface. The adhesion forces become more significant as the particle size decreases, making the particle

harder to remove.¹² For example, the basis of clean room technology was designed to minimize the deposition of fine particles to reduce yield loss during manufacturing of circuits. The current methods of removing sub-micrometer sized particles, or adsorbed contaminants, from a surface are limited by the risk of damages it could cause to the pristine surface beneath.

1.5 SURFACE CONTAMINATION REMOVAL

Common methods of contamination removal involve thermal annealing, UV-Ozone treatment, ion beam etching, and solvent cleaning. Each of these has some effect of influencing the chemistry of the pristine surface. Thermal annealing at high temperatures results in the removal of carbon based contaminants, but also may result in the oxidation of metal surfaces or the formation of surface defects. UV-Ozone operates by utilizing UV light to produce highly reactive ozone. So, when the UV radiation interacts with the sample, adsorbed carbon based contaminants are removed through an oxidative process.²⁰ However, this technique is at risk of oxidizing the pristine sample surface, which could potentially influence wettability. As far as ion beam etching is concerned, bombardment with Ar^+ ions not only removes surface carbon, but also impacts surface chemistry—affecting the oxidation state of metal atoms in particular. This has implications on the wettability of the surface.²¹ Solvent cleaning is a known method to remove adsorbed contaminants on a surface, but has the added issue of leaving behind residue solvent molecules, influencing the chemistry of the substrate.²² Each of these cleaning methods have inherent risks of impacting surface chemistry. While some may be more effective in removing surface carbon than others, they are all at risk of producing changes in surface chemistry. This presents the problem of determining whether a surface is intrinsically

hydrophobic, or if its hydrophobicity is due to contamination on the surface of the substrate, since the act of cleaning the substrate may inherently change the surface chemistry. It is a problem deciphering if the cleaned surface's wettability is its true intrinsic nature, or if the wettability of the cleaned surface was affected by the cleaning process.

1.6 INTRODUCTION TO SURFACE CHARACTERIZATION TECHNIQUES

1.6.1 Atomic Force Microscopy (AFM)

AFM imaging is a technique used to study the morphology of a surface. AFM consists of a cantilever with a sharp-point probe at its end that is used to analyze and scan the heights of the surface beneath it. The radius of this tip is usually on the scale of a few nanometers. When the tip is brought into close proximity to the sample's surface, forces between the surface and the cantilever lead to a deflection according to Hooke's law. This deflection can be measured using a laser reflected from the backside of the cantilever to a series of photodiodes. The AFM has different modes of operation. AC Tapping mode was used to study the morphology of as-received and thermally annealed CeO₂ wafers.

1.6.2 Optical Microscopy

Optical microscopy imaging uses visible light to magnify a sample through a series of lenses of various magnification strengths. Optical images were taken using an AmScope with an

MT camera. Optical microscopy was used to visualize any possible changes in surface morphology between fresh and thermally annealed CeO₂ wafers.

1.6.3 Water Contact Angle

Wetting is the ability of a liquid to maintain contact with a solid surface, resulting from intermolecular interactions when the two surfaces are brought into contact. The degree of wetting can be understood as a balance of forces between adhesive forces, or the interactions between the liquid and solid causing the liquid to spread, and cohesive forces, which cause the liquid to ball up and reduce contact with the surface. The water contact angle, θ , is the angle at which the edge of the droplet contacts with the solid. A contact angle of 0° indicates complete wetting and super hydrophilicity, a contact angle between 0° and 90° , or high wettability, indicates a hydrophilic surface. The interactions between the liquid and solid surface are very favorable, so the liquid will spread. On the other hand, a contact angle between 90° and 180° indicates low wettability, or a hydrophobic surface. And lastly, a contact angle greater than 180° indicates complete non-wetting, or a super hydrophobic surface. High contact angles above 90° occur when the interactions between the liquid and solid surface are unfavorable, so the liquid minimizes contact with the surface, forming a more complete spherical droplet. WCA measurements were taken for as-received and prepared CeO₂ wafers, Dy₂O₃ foils, and Gd₂O₃ foils.

1.6.4 X-Ray Photoelectron Spectroscopy

X-Ray Photoelectron Spectroscopy (XPS) is a quantitative surface analysis technique which measures the elemental composition of a samples surface. XPS spectra are obtained by irradiating a sample with a beam of X-rays, while simultaneously measuring the kinetic energy of electrons escaping from atoms within the first few nanometers of the surface. An elemental composition of the top 1-10nm of the surface is therefore able to be acquired through this method. Relative ratios of atomic species are compared to all analyzed atoms in the entire depth of analysis, not just the top layer of the surface of the substrate. XPS requires high vacuum (at least 10^{-8} mBar) for proper operation and analysis. XPS is able to be implemented with other techniques for further analysis, such as ion beam etching (depth profiling). For such a technique, a sample surface is exposed to an Ar^+ ion beam, which etches, or removes, top layers of the substrate. The size and strength of the ion beam can be controlled, which affects the etching rate of the surface. Additionally, the chemical composition of the substrate also affects the rate of etching. Taking this into consideration, ion beam etching can be implemented to remove contamination layers, or expose layers beneath the surface. Combining this with XPS, one can study how the surface chemistry changes after sequential removal of surface layers of the substrate. XPS was used to analyses as-received and treated CeO_2 wafers and Dy_2O_3 foils, as well as implementing Ar^+ ion beam etching to remove surface contamination.

2.0 EXPERIMENTAL METHODS

2.1 MATERIALS

Gadolinium and Dysprosium foils were obtained from Strem Chemicals Inc. The Cerium oxide thin film on Si wafer used in this study was donated by Dr. Kripa K. Varanasi from the Massachusetts Institute of Technology. The tube furnace used to anneal the REO samples was Lindberg Blue M from Thermo Scientific. UV-Ozone treatment was performed using a Bioforce nanosciences UV/Ozone ProcleanerTM. Deionized (DI) Water used for WCA measurements and solvent washing was from Milli-Q Millipore Advantage 10 filtration system. Acetone (CHROMASOLV Plus, for HPLC, $\geq 99.9\%$) for solvent washing was purchased from Sigma Aldrich. 1-Octadecene, $\geq 95\%$, was purchased from Sigma Aldrich.

2.2 SAMPLE PREPARATION METHODS

2.2.1 Sample Transport

Any transport of freshly cleaned samples (eg. Thermally annealed, UV-Ozone treated, or sputtered) with uncontaminated pristine surfaces was performed by placing the samples in sealed glass containers flushed with pure N₂ gas. It is important to note that these containers were first cleaned with UV-Ozone for 20 minutes to remove any adsorbed hydrocarbons on the surface of the glass.

2.2.2 Thermal Annealing

Gadolinium and Dysprosium samples were thermally annealed at 1050°C for 1 hour in air, 30 minutes of which was a ramp-up period of the oven reaching the desired temperature. Samples of CeO₂ thin film were annealed at 300°C, 500°C, and 800°C. Samples were annealed for 1 hour at the desired temperature; with a 10, 15, and 20 minute ramp period, respectively.

2.2.3 UV/Ozone

REO samples were treated by UV-Ozone for 20 minutes to remove any surface hydrocarbon contamination. Before UV treatment, the UV/Ozone chamber was flushed with pure O₂ gas to encourage the oxidative UV-Ozone process. After 20 minutes of UV/Ozone

exposure, the instrument was then flushed with N₂ gas, to remove O₃, before removal of the sample.

2.2.4 Ar⁺ Sputtering

Ce₂O₃ samples were sputtered using an Ar⁺ ion beam with energy of 200eV for 5-10 seconds, depending on the initial level of carbon contamination, measured by XPS. This was done to remove the carbon contamination from the surface of the sample layer while avoiding etching into the actual oxide layer.

2.2.5 UHV Storage

Ce₂O₃ samples were kept under ultra-high vacuum (UHV) in the XPS analysis chamber during the entire storage time. UHV pressure during storage was steady at 7×10^{-10} Torr, with the pressure reducing to 3×10^{-7} only during measurements. This storage technique allowed for immediate analysis of UHV storage effects since the sample was stored in the UHV analysis chamber of the XPS.

2.2.6 Solvent Cleaning

Ce₂O₃ samples were cleaned with acetone, followed by DI water. Acetone washing utilized a plastic wash bottle for a slightly aggressive stream. DI water washing used a large

glass pipette cleaned with UV/Ozone, to ensure minimal hydrocarbon contamination. Washing times were controlled using a timer.

2.3 CHARACTERIZATION METHODOLOGY

2.3.1 XPS Methodology

In order to determine the surface chemistry and quantify hydrocarbon contamination, X-Ray photo electron microscopy (XPS) measurements were taken with a Thermo Scientific™ ESCALAB 250Xi. X-Ray source was monochromatic and used an Al anode. Spot size was 0.4mm with an angle of 45°. Freshly annealed samples were immediately transferred from the thermal annealing oven to the XPS using a sealable glass container in order to prevent adsorption of airborne contaminants. Before transfer, the glass container was cleaned via UV-Ozone treatment for 20minutes in order to ensure minimal hydrocarbon contamination from the inside surface of the glass; additionally, glass containers were flushed/filled with pure N₂ gas after the samples were introduced. It is important to note that glass joint grease was avoided, as to prevent possible airborne contamination within the transfer container. Transfer time of the sample to the XPS preparation vacuum chamber was kept minimal (<5min), with the sample only being in the XPS preparation chamber for less than 10 minutes. This method provided minimal air exposure to the sample, reducing possible sources of airborne contamination.

In order to ensure precise measurements, minimal of 10 scans were taken for each elemental measurement. Measurements were acquired, peak deconvoluted, and analyzed using the powerful Thermo Scientific™ Avantage Data System software. Peak fitting allowed for Lorentzian-Gaussian ratio control as well as difference spectra optimization, with the Shirley method being implemented to calculate the background spectrum.

XPS-stored samples were kept under ultra-high vacuum (UHV) in the XPS analysis chamber during the entire storage time. UHV pressure during storage was steady at 7×10^{-10} Torr, with the pressure reducing to 3×10^{-7} only during measurements.

2.3.2 WCA Methodology

WCA measurements were conducted using a VCA Optima XE contact angle system at room temperature (22°C). Water droplets were 2 μ l in size and suspended on the tip of the instrument needle. The sample surface was raised up to carefully touch the bottom of the water droplet. Static contact angle measurements were calculated using the VCA Optima XE software, with images captured by a charge-coupled device (CCD) camera. Each measurement was repeated three times and the average WCA value was reported.

Samples were stored in open UV/O cleaned glass vials. It is important to note that the samples were not vertically exposed to the ambient air—the glass vials were placed horizontally to allow the free flow of airborne molecules and to prevent any particles from landing directly onto the sample's surface. This setup essentially guarantees any WCA influence is solely from the effect of adsorbed molecules onto the sample's surface.

2.3.3 Optical Microscopy Methodology

Optical images were taken using an AmScope with MT camera with the vendor-supplied software.

2.3.4 Atomic Force Microscopy Methodology

The AFM measurements were taken using an Asylum MFP3D AFM in AC Air Tapping Mode using silicon tips with a resonance frequency of 320kHz. Analyses were performed using the vendor-supplied software.

3.0 WETTABILITY AND RARE EARTH OXIDES

Many applications require materials that are both intrinsically hydrophobic and robust. Examples of such applications range from anti-icing coatings for aircrafts to preventing condensation buildup on heat exchangers.²³ The current technology in hydrophobic coating is limited to organic materials that are easily degraded and require lengthy process to apply and maintain. A study by Azimi *et al.* suggested that REOs are intrinsically hydrophobic (WCA of 115°) because their electronic structure prohibits their bonding with interfacial water (**Figure 4**).²⁴ This is a potentially transformative discovery because metal oxides are much more robust than organic coatings, and therefore could be used in a much wider range of applications. However, the hydrophobicity of REOs is also quite unexpected because all other metal oxides are known to be super-hydrophilic in their pristine states. In addition, given that rare-earth metal ions bind water strongly in aqueous solution, and bulk the REO surface strongly adsorbs water, it is puzzling why REOs surface would be hydrophobic.

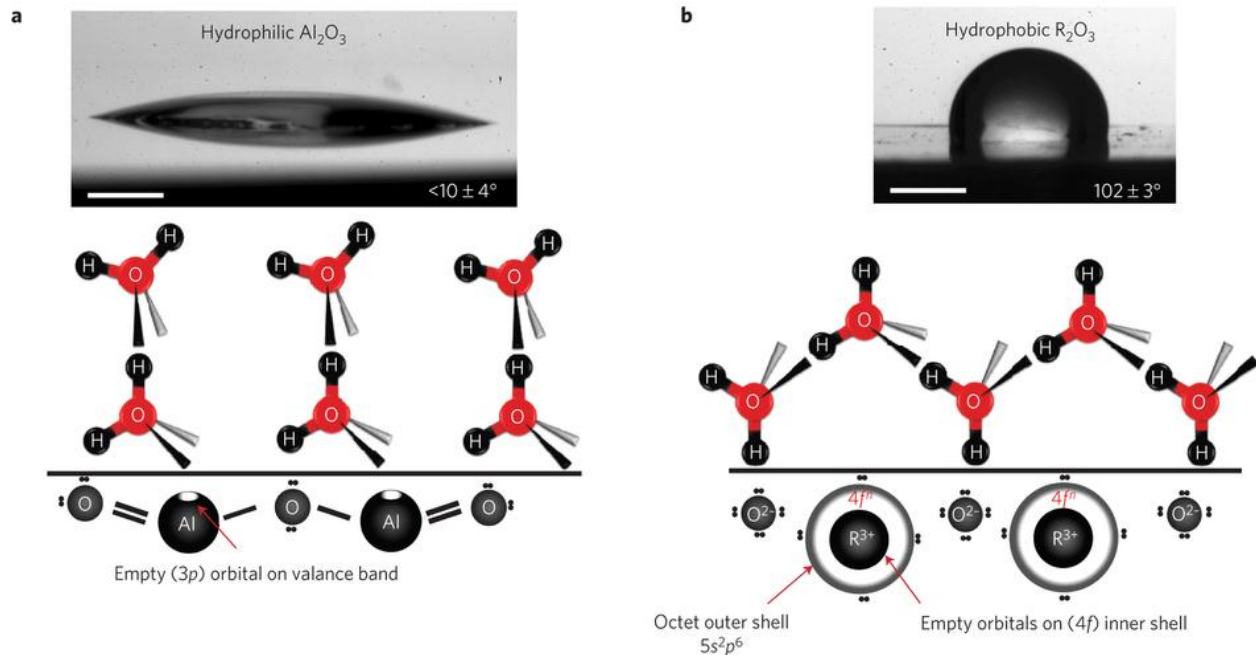


Figure 4. Schematic of the orientation of water molecules and the associated wetting properties of a surface. (a) Hydrophilicity and schematic of the orientation of water molecules next to an alumina surface (using different scales for the surface and water molecules). (b) Hydrophobicity and schematic of the orientation of water molecules next to neodymia (an REO) (surface and water molecules not to scale). Scale bars, 1 mm. Reprinted with permission from Azimi et al., Nat. Mater. 12, 315 (2013). Copyright 2013 Macmillan Publishers Limited.

Azimi *et al.* suggested that the hydrophobicity of REOs is due to the $4f$ orbitals of rare-earth atoms being completely shielded by the octet electrons of the outer ($5s^2p^6$) orbitals, and therefore have no tendency to interact with water molecules.²⁴ Due to this factor, they suggested that water molecules next to the surface would not be able to maintain the hydrogen bonding network, and would therefore be expected to have a hydrophobic surface. This property is unique to the electronic structures of REOs. The only method to validate or disprove this is would be experimentally. As noted in Section 1.4, a hydrophilic surface is expected for CeO_2 , and all REOs, given the high lattice energies of these materials.

Additionally, they have shown in further studies that freshly sputtered surfaces (CeO_2 thin film on Si wafer), contain extra surface oxygen, which influence surface measurements.

When these surfaces are relaxed in a *clean*, ultra-high vacuum environment *isolated from airborne contaminants* they reach close to stoichiometric O:Ce ratio (2.2) and becomes hydrophobic (WCA of 104°). However, these studies were not performed in a *clean* UHV chamber *isolated from contaminants*. The carbon content associated with the WCA of 104° was reported to be 12.7%.²⁵ This value is extremely high, and will be shown to correlate to very high WCA when compared to lower carbon ratios.

Herein, it is proven that REOs are intrinsically super-hydrophilic and the hydrophobicity observed by Azimi *et al.* was due to airborne hydrocarbon contamination. Airborne hydrocarbons concentrations typically range in the parts-per-trillion to parts-per-billion level.¹⁸ It is also proven that UHV storage is not void from contaminants, and does not prevent carbon contamination. Any WCA or surface measurements must not avoid this vital issue. The timescale of such adsorption process can range from several minutes to several weeks, depending on the nature of the surface and the local concentration and identity of airborne hydrocarbons.¹⁹ For high energy surfaces, this hydrocarbon adsorption results in an increase of their water contact angle (WCA), by strongly reducing the surface free energy, and vice versa.¹⁹

4.0 RESULTS AND DISCUSSION

4.1 WETTABILITY OF GADOLINIUM AND DYSPROSIUM (REOS) FOILS

The results show that a clean REO surface is super-hydrophilic but becomes hydrophobic when contaminated by airborne hydrocarbons. To demonstrate this, the wettability of Gd_2O_3 and Dy_2O_3 surfaces was studied as a function of their surface chemistry. The WCA of an as-received Gd foil, which has a native Gd_2O_3 layer, was 97° (**Figure 5a**). Such a large WCA suggests hydrophobic behavior and is also consistent with the value reported by Azimi *et al.*² To remove any possible adsorbed hydrocarbons on the surface, Gd foil was annealed in air at 1050°C for 1 hour. In addition to removing the adsorbed hydrocarbon, the high temperature treatment also converted surface Gd to Gd_2O_3 .¹⁶ Immediately after the annealing, the sample exhibited super-hydrophilic behavior, giving a WCA of 0° (**Figure 5a**), measured within 2 min of annealing. However, upon exposure to ambient air, the WCA gradually increased over time and plateaued at *ca.* 84° after 10 hours (**Figure 5a-b**). Similar change of wettability was also observed on Dy_2O_3 samples: a Dy_2O_3 substrate showed 0° WCA immediately after annealing at 1050°C and the WCA increased to 66° after 12 hours of exposure to ambient air. To verify that it is airborne hydrocarbon that is responsible for the observed wetting transition, 1-octadecene ($\text{C}_{18}\text{H}_{36}$, ODE)

vapor was introduced to the Gd_2O_3 sample and observed that the WCA increase was drastically accelerated (**Figure 5b inset**). In another experiment, it was found that storing an annealed and partially air-contaminated Gd_2O_3 sample inside a plastic bag for a few minutes could result in an immediate increase of its WCA from 40° to 85° . All these data strongly suggest that the previously observed hydrophobicity of REOs is entirely due to airborne hydrocarbon contamination.²⁴

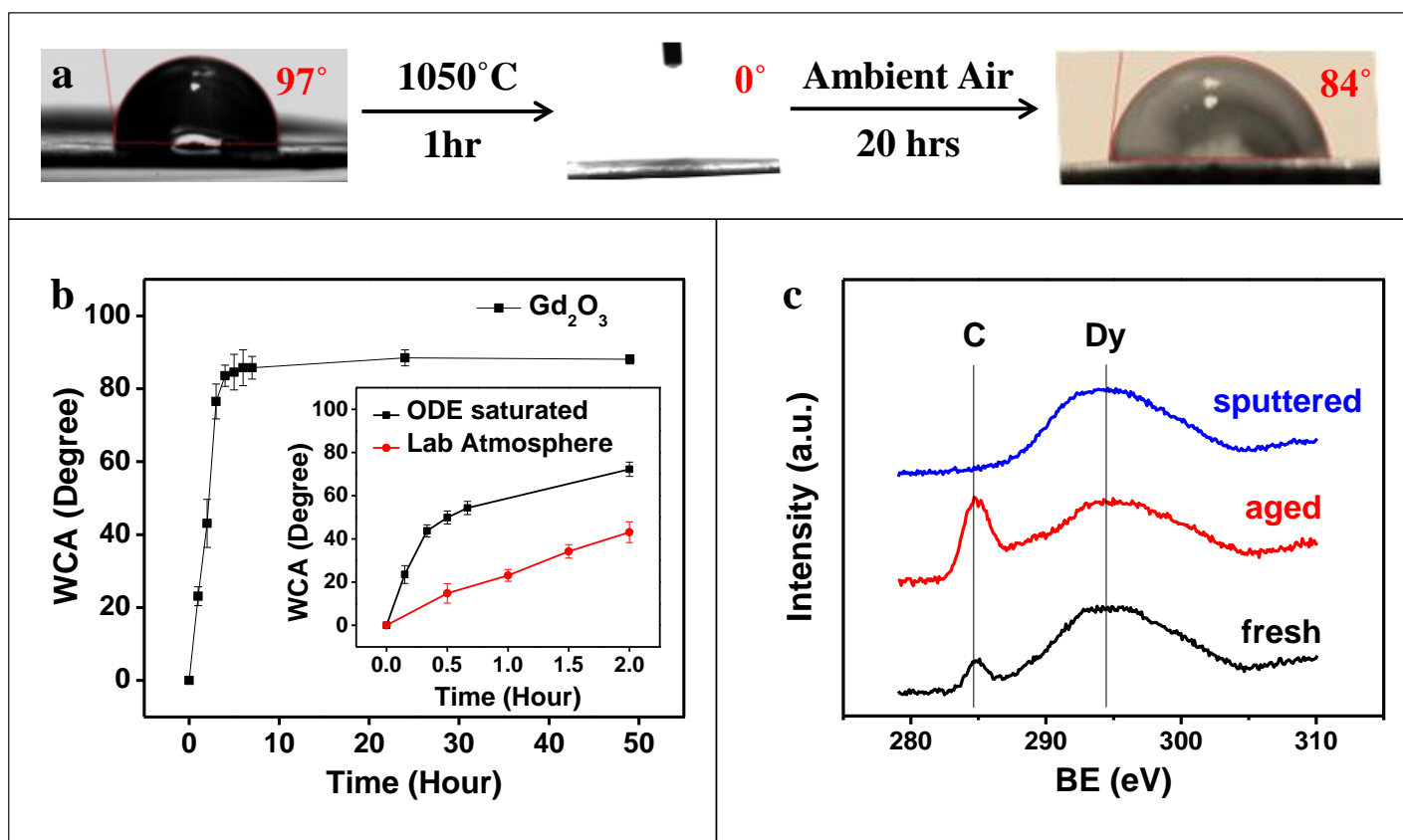


Figure 5. Time Evolution of Air Exposed REOs | (a) Effect of thermal annealing and air exposure on the wettability of a Gd_2O_3 substrate. **(b)** WCA of Gd_2O_3 substrate as a function of air exposure time. The inset shows the effect of ODE vapor on the time evolution of the WCA. **(c)** XPS spectra of fresh, aged (3 months), and Ar^+ ion sputtered Dy_2O_3 substrate. BE: binding energy.

The surface contamination by airborne hydrocarbons was further verified by X-ray photoelectron spectroscopy (XPS). For these experiments, a Dy foil was annealed in air at 1050°C for 1 hour to form a thin layer of Dy₂O₃. Upon removal from the annealing chamber, the foil was transferred to an XPS for measurement. The first XPS spectrum was collected within 5 minutes of ambient air exposure and 20 minutes of exposure in the vacuum environment of the XPS chamber. The sample was then taken out of the XPS chamber and exposed to ambient air for a fixed amount of time before additional XPS spectra were taken. **Figure 5c** shows the C1s and Dy4p₃ region of the XPS spectra. As can be seen, the carbon peak increased after exposure to ambient air. The C:Dy atomic ratio was 1:32 in the freshly annealed sample and increased to 1: 8.9 after exposing to air for 2 months. To verify that the carbon peak was indeed due to the adsorbed hydrocarbon on the surface, the surface was sputtered with Ar⁺ ions and observed an immediate disappearance of the C1s XPS peak (**Figure 5c**).

4.2 WETTABILITY OF CERIUM OXIDE THIN FILM

The CeO₂ sample used in this study was prepared via sputtering deposition on a silicon wafer and stored in air for several weeks prior to analysis. The CeO₂ thin film wafer was donated by Dr. Varanasi from MIT. The as received sample gave a WCA of 98.7° and XPS analysis showed that there was 21.85% of carbon on the surface. It is noted that the XPS measurements only sets a lower bound of the surface contamination as a significant amount of adsorbed hydrocarbons will desorb in high vacuum. Overall, these results clearly indicate that REO surfaces are capable of adsorbing significant amount of hydrocarbon from air. It is important to note that a study from the Varanasi lab reported *ca.* 12% of carbon on a CeO₂ sample that was stored briefly in a vacuum desiccator.

In Azimi *et al.*, the REO samples were stored in a vacuum desiccator for an undisclosed amount of time before their wettability was tested. Storing samples in a vacuum desiccator may expose them to high level of hydrocarbons from vacuum grease, plastic parts (*e.g.*, rubber vacuum hose), and back-diffused pump oil vapor. As will be shown below, hydrocarbon contamination even occurs on samples stored in an ultra-high vacuum (UHV) environment. It is therefore speculated that the REO samples of Azimi *et al.* may have been contaminated prior to their wettability test. Although XPS data was presented in Azimi *et al.*, and low carbon contents were reported for the REO samples, such data were collected after the surfaces were cleaned by Ar⁺ sputtering and therefore do not support the absence of hydrocarbon contamination.

To obtain a clean CeO₂ surface, samples were thermally annealed to oxidize and remove the adsorbed hydrocarbons. It was found that annealing the sample at 300 °C resulted in incomplete removal of hydrocarbon, while annealing at 800 °C produced crack lines in the sample (**Figure 9**). For the sample annealed at 500 °C for 45 minutes, no crack or damage was observed by optical microscopy and atomic force microscopy (AFM). A carbon content of 4.75% was measured by XPS and the WCA data measured immediately after the annealing was 0° (**Table 2 #2 and Figure 6**). When stored in ambient air, XPS analysis showed an increase of carbon content on the surface and the WCA also slowly increased. The WCA was 56.3° after 24 hours of aging in air, and ultimately reached 65.6° after 2 weeks (**Table 2 #3-#4 and Figure 8**). This result shows that CeO₂ surface is hydrophilic after removing hydrocarbon contaminant and re-adsorbs hydrocarbon when exposed to air. Similar observations were also made using Gd₂O₃ and Dy₂O₃ samples prepared by annealing the corresponding metal foils in air.

Because thermal annealing could introduce stress on surface, the effect of potential surface relaxation on the wettability was tested. In this experiment, the sputtered CeO₂ sample was thermally annealed (500 °C, 45 min) and then stored in an ultra-high vacuum (UHV) chamber (7×10^{-10} Torr) for 24 hours to relax the surface. The surface carbon content increased slightly (from 4.75% to 7.01%) during the UHV aging, likely due to the adsorption of residual hydrocarbon in the UHV chamber (**Table 2 #5 and Figure 6**). The WCA measured immediately after the UHV aging was 33.1°. Further storage in ambient air resulted in additional increase in the WCA, reaching 65.8° after 2 weeks (**Table 2 #6 and Figure 6**). This data shows that surface relaxation, if any, does not significantly impact the wettability of CeO₂.

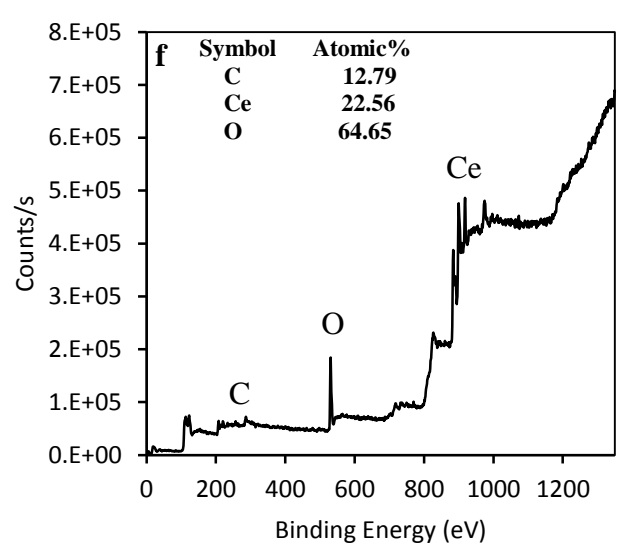
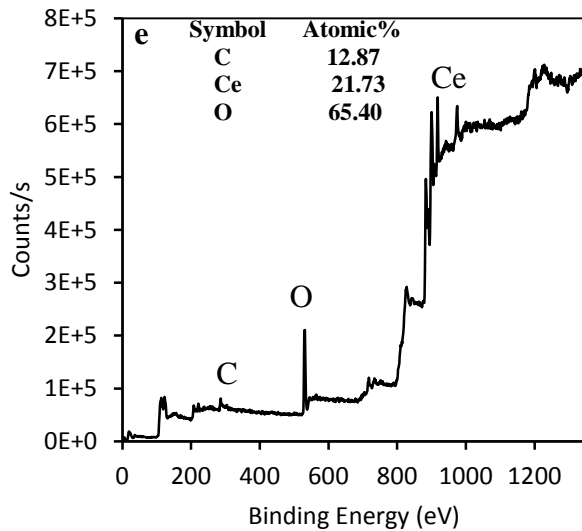
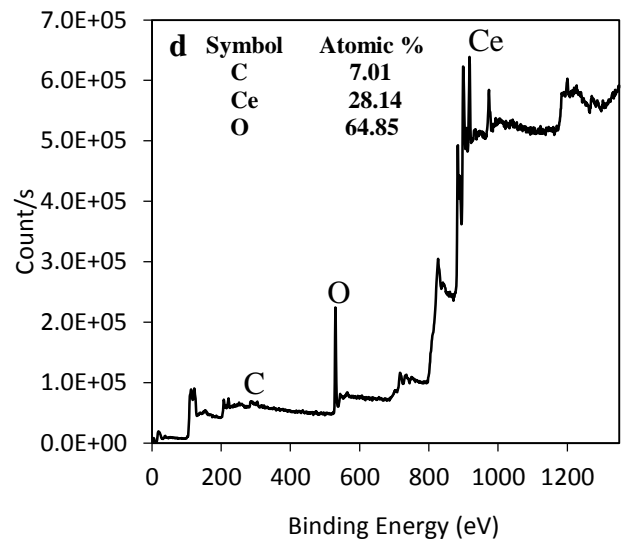
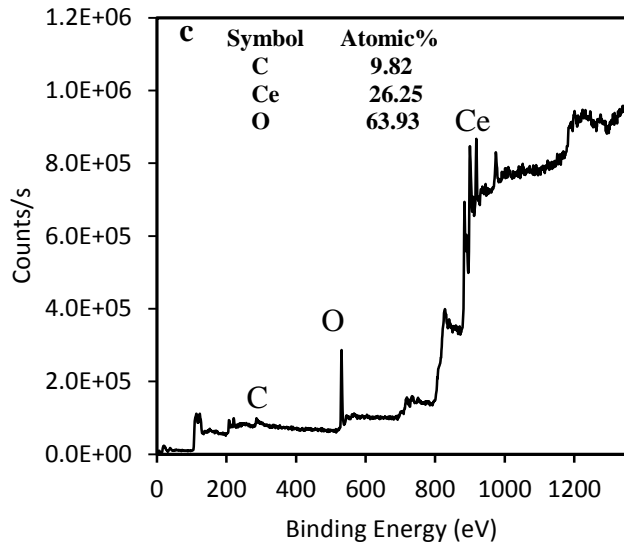
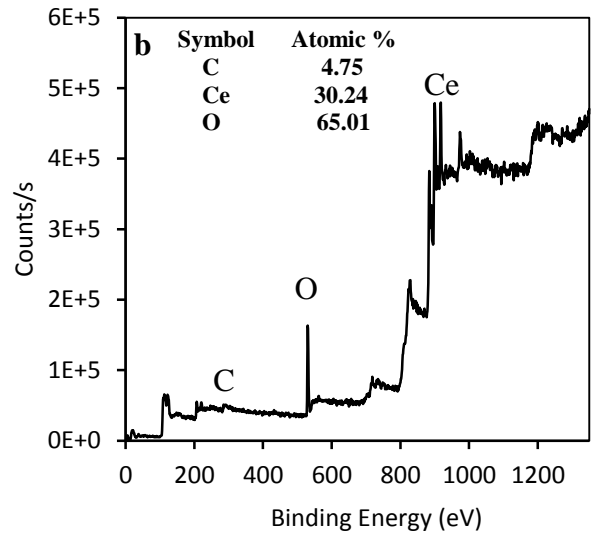
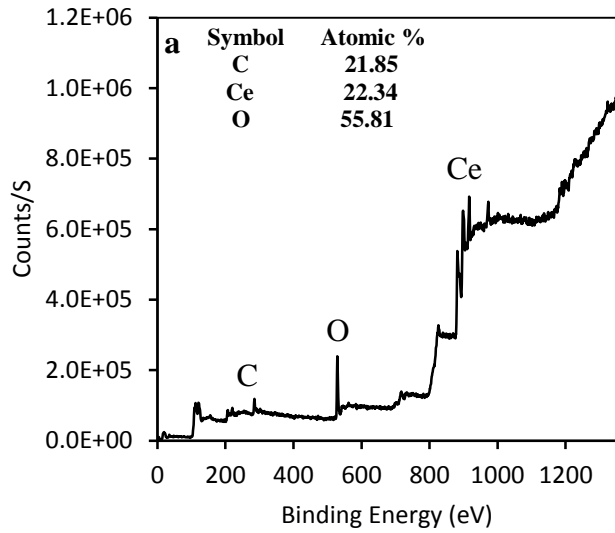
CeO₂ samples were also cleaned by utilizing other methods. Samples were treated with UV/Ozone, Ar⁺ sputtering, and cleaned with solvents. Similar trends were observed with these

cleaning methods as with thermal annealing. When stored in ambient air, XPS analysis showed a correlating increase of carbon content with WCA. Since these cleaning methods, in addition to thermal annealing, may produce defects, the surface chemistry was analyzed for changes before and after treatment (**Figures 11-15**). No substantial defects were observed.

It was found that exposing the sample to UV/Ozone removes substantial surface carbon. After 20 minutes of treatment, a carbon content of 4.61% was observed, with a WCA of 0° (**Table 2 #7** and **Figure 6**). Transport time between the portable UV/Ozone instrument to the XPS, when compared to transport from the thermal annealing oven, was about 50% faster. This fast transfer reduces the time for airborne contaminants to adsorb to the surface. The time evolution of WCA was 47.7° after 24 hours of aging in air, and ultimately progressed to 62.98° after 2 weeks (**Figure 7**). Ar^+ sputtered CeO_2 film resulted in in a carbon content of 0 with a WCA of 0° (**Figure 6** and **Table 2 #8**). The WCA increased to 51.16° after 24 hours of air exposure, and ultimately reached 60.95° after 2 weeks, with corresponding increase in carbon content (**Figure 7**).

Solvent cleaning of CeO_2 was also performed. Samples were cleaned with acetone (10seconds) followed by DI water (10 seconds). This was followed by fully drying in air. The WCA of the sample reduced from 99.4° (pre-wash) to 66.39° after washing (**Table 2 #10**). This correlated with a carbon content reduction of 25.42% (**Table 2 #9**) to 18.27%, after washing (**Table 2 #10**). Solvent washing was also performed for longer periods (60 seconds acetone, 60 seconds DI). However, longer washer periods produced identical WCA and %C reduction as washing for 10 seconds. Additionally, washing an aged sample with only DI water produces no reduction in WCA. Aged samples were rinsed with DI for 1 minute, than soaked in DI water for 1 minute (no acetone). No reduction of WCA (99°) or carbon content was observed. This

indicates that DI water is not a proper solvent to remove surface contaminants, but also that DI water will not chemically alter the surface of the CeO₂ substantially, if at all, to affect wettability.



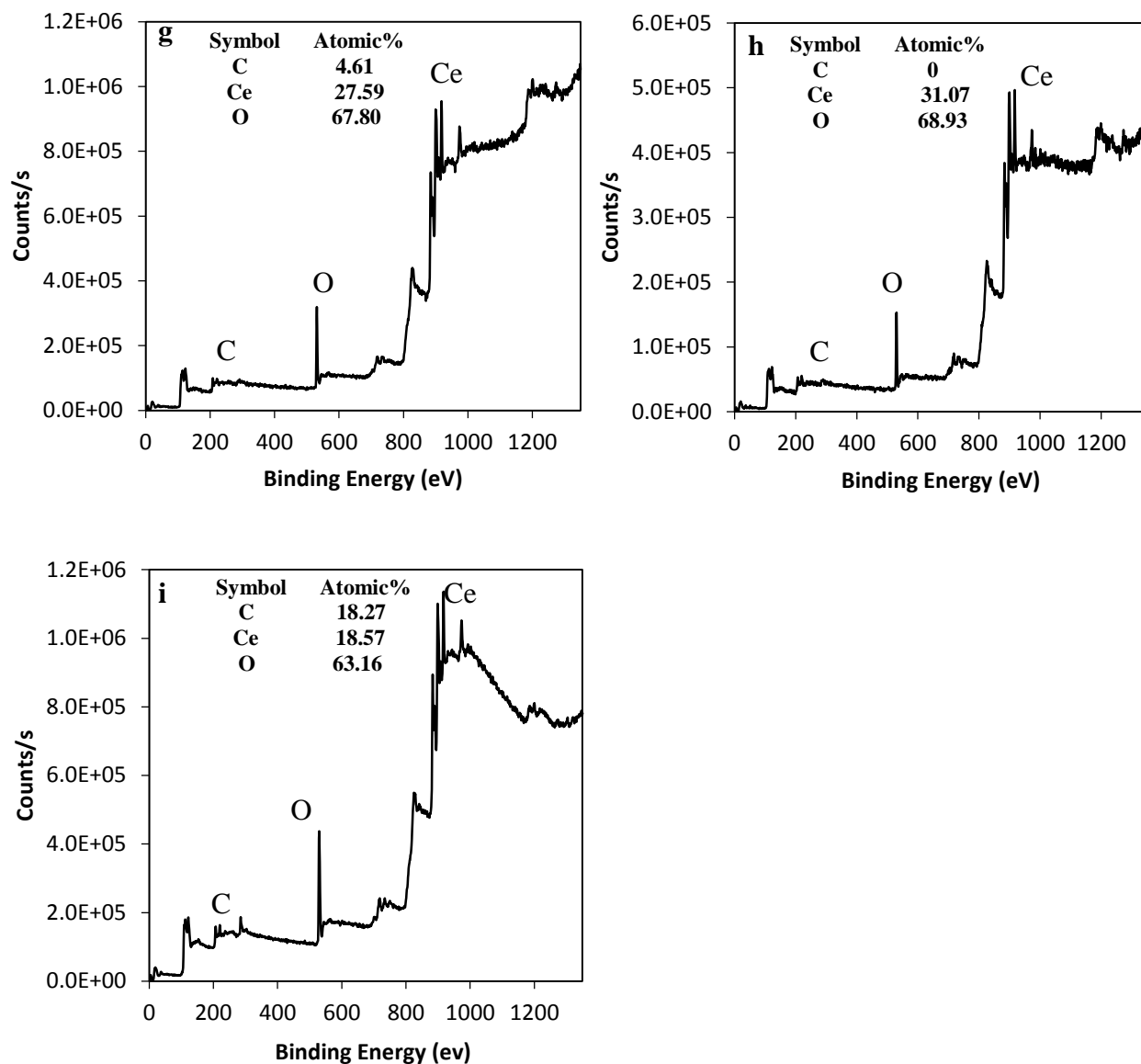


Figure 6. XPS Spectra of as-received and treated CeO₂ thin films. | **a**, As received; **b**, Freshly annealed at 500°C; **c**, Sample A stored in ambient air for 24 hours; **d**, Sample A stored in UHV XPS chamber for 24 hours; **e**, Sample C stored in ambient air for 2 weeks; **f**, Sample D stored in ambient air for 2 weeks; **g**, Sample A treated with UV/Ozone for 20 minutes; **h**, Sample A sputtered with an Ar⁺ ion beam; **i**, aged CeO₂ (25.42% C) sample washed with acetone (10s) followed by DI water (10s).

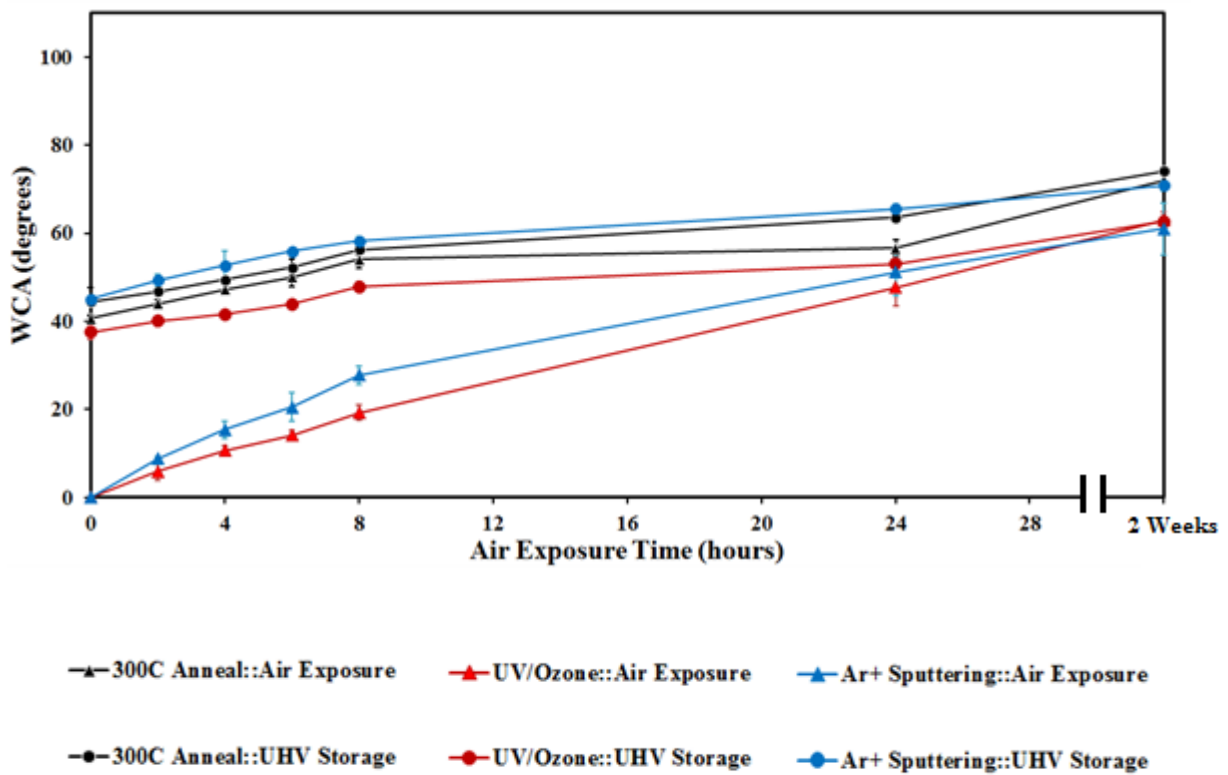


Figure 7. WCA of Treated CeO₂ films | Samples were cleaned using three different methods. Clean samples were then either immediately exposed to air (triangle) or first exposed to 24 hours of UHV (circle). The time evolution of the WCA plotted after cleaning, with the first point indicating the start of air exposure. Black; Samples were annealed at 300°C for 1hour. Red; samples were cleaned using UV/Ozone for 20 minutes. Blue; Samples were sputtered using an Ar⁺ ion beam at 500eV for 5 seconds.

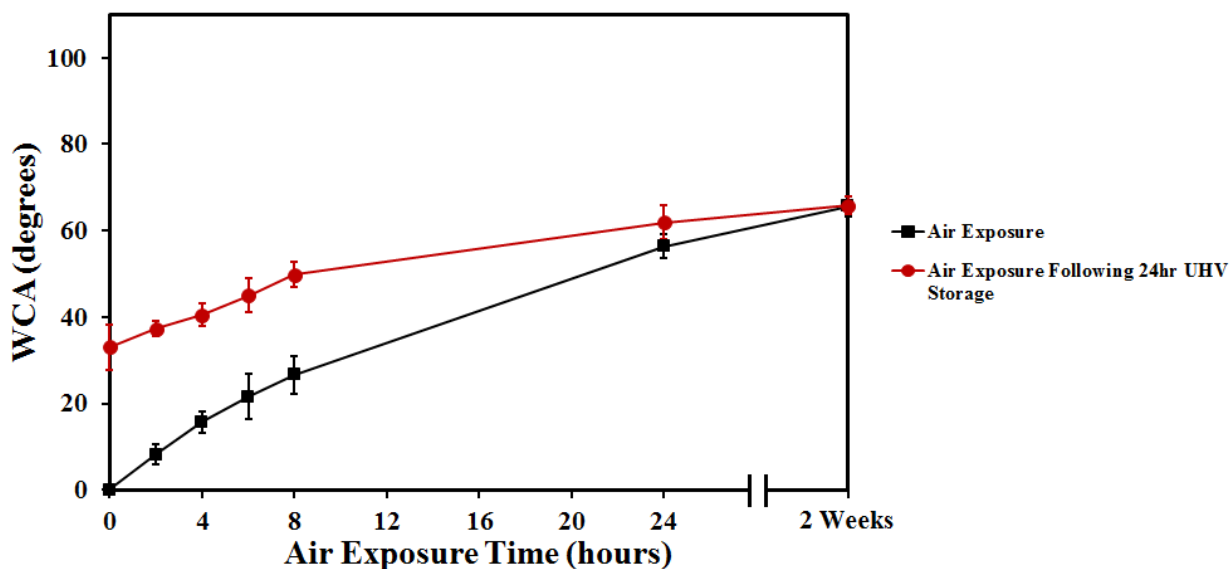


Figure 8. WCA of CeO₂ thin films annealed at 500°C | Samples were prepared by annealing for 45 minutes at 500°C with a 15 minute temperature ramp. **Black**, Immediate air exposure after annealing with corresponding WCA measurements; **Red**, Sample stored in UHV (7×10^{-10} Torr) for 24 hours, followed by storage in ambient air. First measurement (0 hours of air exposure) is taken immediately after UHV storage.

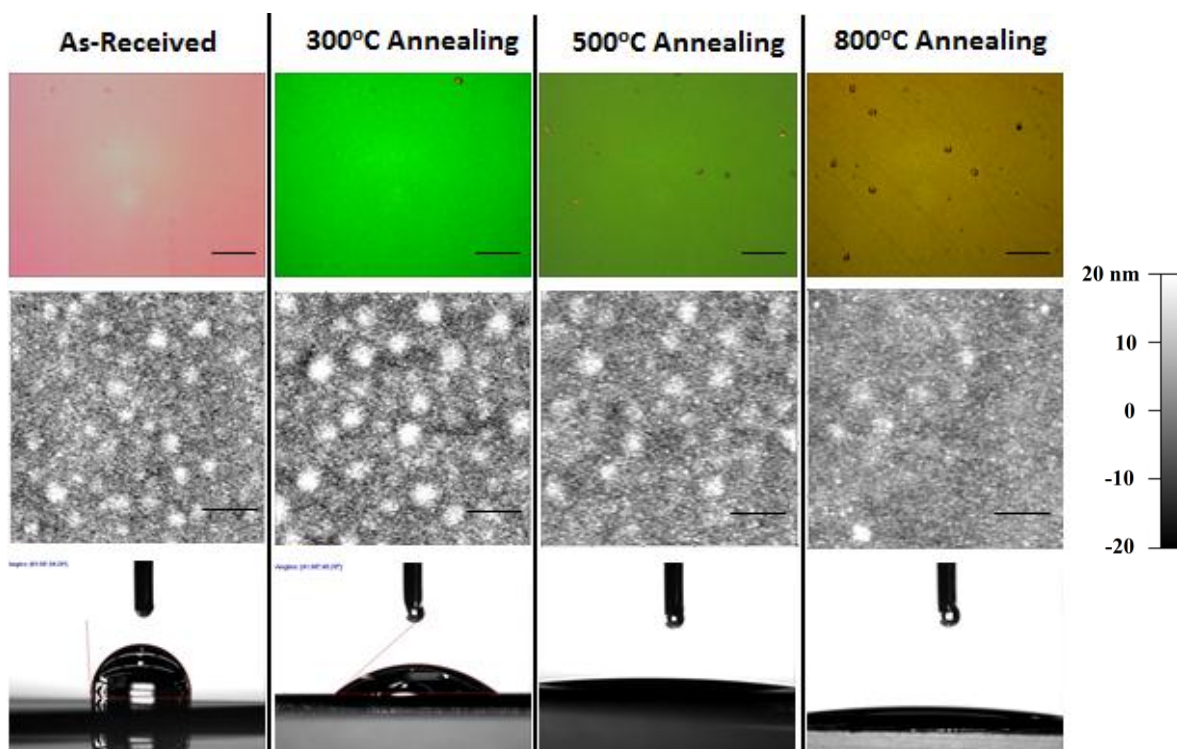


Figure 9. Surface Morphology Characterization of annealed CeO₂ Thin Films | Optical micrograph (top; scale bar: 50 μm), AFM (middle; scale bar: 2 μm), and WCA measurements of CeO₂ samples. Surface cracks in CeO₂ film were only observed in sample annealed at 800 °C. The difference in the color is due to variation in the thickness of CeO₂ film—pink-green color variations are seen in the as received untreated sample.

Table 2. WCA and Surface Carbon Content of CeO₂ Samples

#	Treatment	WCA (degree)	%C
1	As received CeO ₂ thin film on Si wafer	98.7	21.85
2	Thermal annealed Samples at 500 °C	0	4.75
3	Sample 2, aged in air for 24 hr	56.3	9.82
4	Sample 3 after an additional aging in air for 2 weeks	65.6	12.87
5	Sample 2, aged in UHV for 24 hr	33.1	7.01
6	Sample 5 after an additional aging in air for 2 weeks	65.8	12.79
7	Sample 1 treated with UV/Ozone for 20 minutes	0	4.61
8	Sample 1 sputtered with Ar ⁺ ions	0	0
9	As received, CeO ₂ thin film on Si wafer	99.4	25.42
10	Sample 10 washed with solvents	66.4	18.27
11	CeO ₂ pellets (Azimi <i>et al.</i>)	103	15.10

Additional evidence of hydrocarbon contamination in Azimi *et al.* It is important to note that Azimi *et al.* also conducted thermal annealing experiments and observed that the hydrophobicity of REO was *maintained* after such treatment. For example, the authors coated CeO₂ film onto silicon microposts and after annealing in air at 500 °C for 2 hours, they observed significant damage on the CeO₂ film. Despite such damage, a WCA of 125° was observed by Azimi *et al.*, in stark contrast to the 0° value reported here. The difference in these results shows that the samples used by Azimi *et al.* were contaminated. In this work, hydrocarbon contamination was minimized by measuring WCA immediately after the annealing treatment.

4.3 SURFACE DEFECT ANALYSIS (XPS)

The cleaning methods mentioned in this work are at risk of producing defects or altering the chemistry of the surface of treated samples. In order to analyze the possible effects that these methods have, XPS analysis was performed on the Cerium peak. Ce(III) and Ce(IV) each have characteristic peaks in the Ce XPS spectra—Ce(III) and Ce(IV) have different binding energies, and therefore peaks. In theory, it is possible to determine the ratio of Ce(III) to Ce(IV) on the surface of a sample. However, the actual quantification of this produces issues, since there is substantial overlap between the two spectra for the peak at 898eV (**Figure 10**).

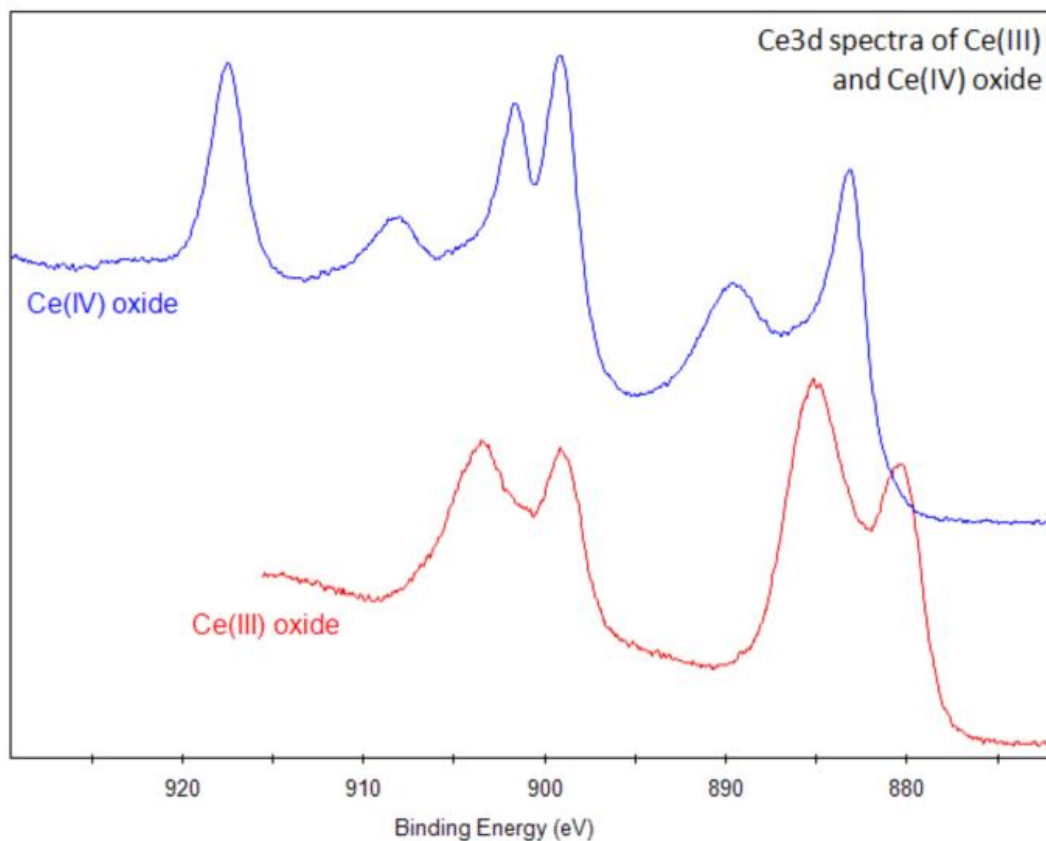


Figure 10. Ce3d_{3/2,5/2} XPS Spectra of Ce(IV) oxide (BLUE) and Ce(III) oxide (RED)²⁶ Measured spectra of CeO₂ (Figures 10-16) are convolutions of Ce(IV) and Ce(III) spectra. Image gathered from Thermo Scientific™ Avantage Data System software.

Cerium peak XPS analysis was still performed on all the cleaned samples (Figures 11-15). In each case, insignificant change was observed between the Ce(IV) and Ce(III) states between the as-received (Figure 11) and treated samples (Figures 12-17). Only a slight reduction of the Ce(III) state was observed in each preparation method. The sample, as received by the Varansi group, contained an inhomogeneous CeO₂ film thickness (as observed by the color gradient on the sample surface). So, precise quantification between samples is virtually impossible.

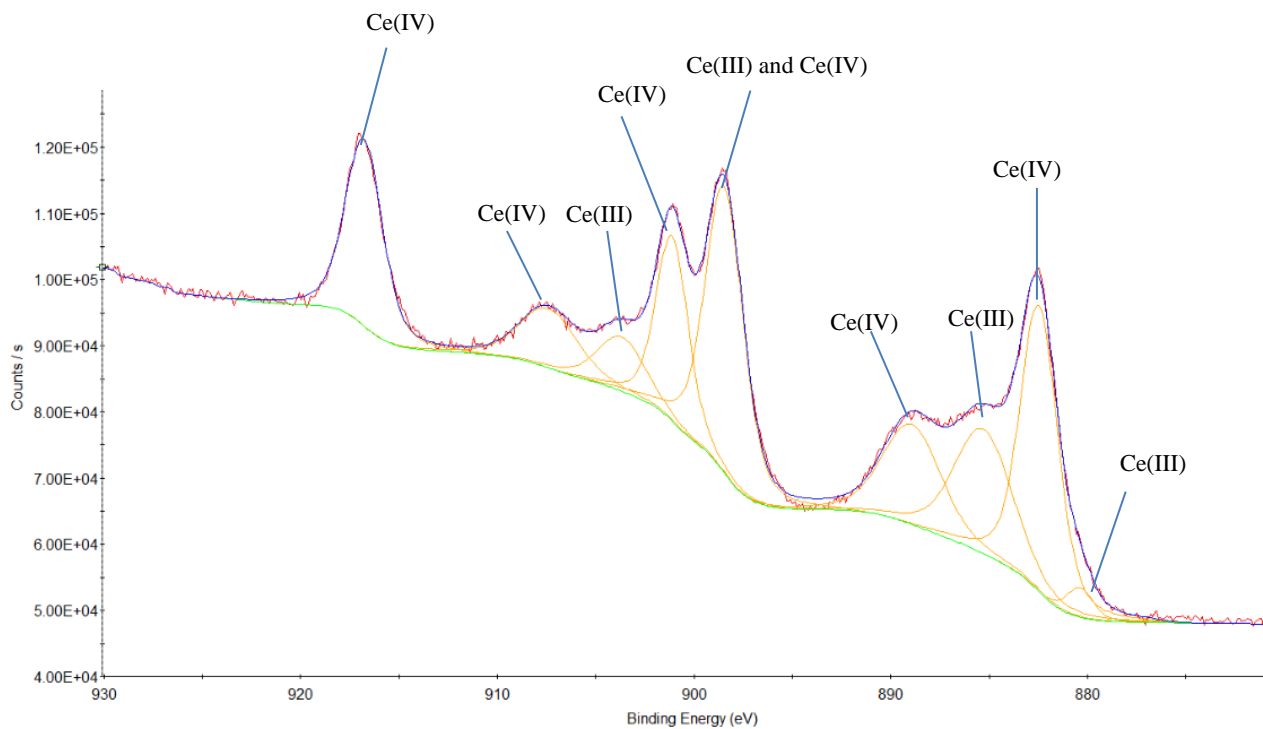


Figure 11. Cerium XPS spectra of as-received, untreated, CeO₂ thin film. Particular peaks are labeled to indicate from which species each peak arises.²⁴ Image gathered from Thermo Scientific™ Avantage Data System software.

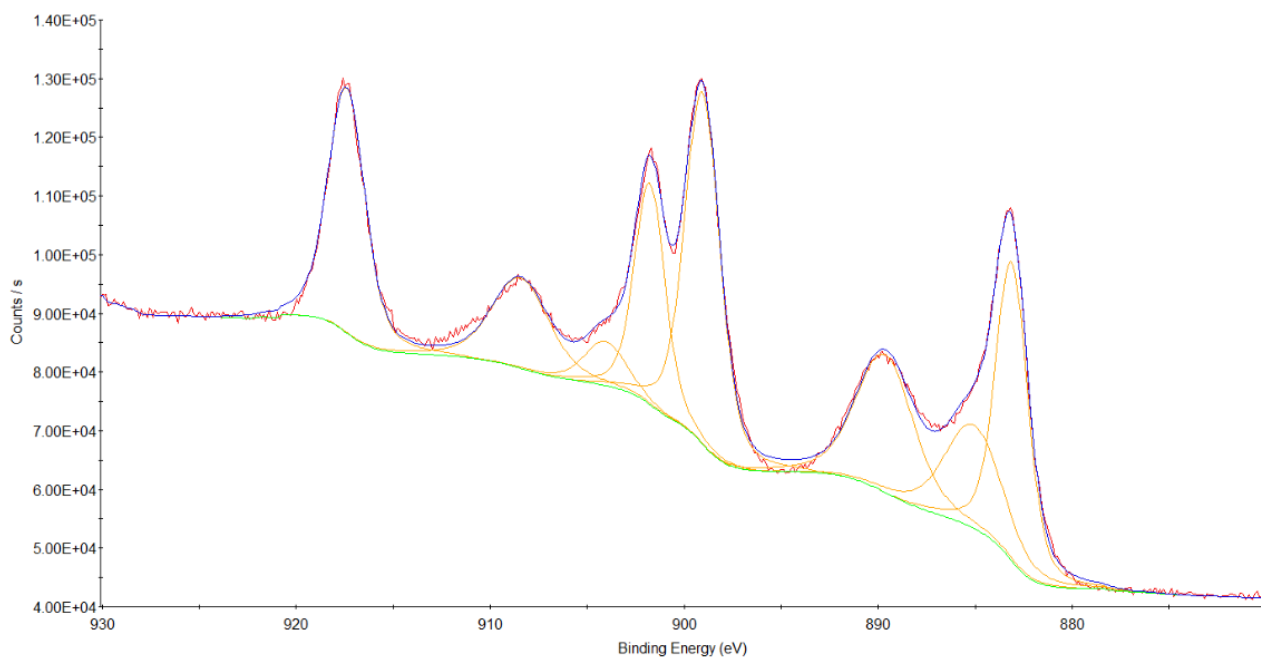


Figure 12. Cerium XPS spectra after 500°C annealing for 1hr. Slight reduction of Ce(III) peak is observed in comparison to untreated samples. Image gathered and analyzed with Thermo Scientific™ Avantage Data System software.

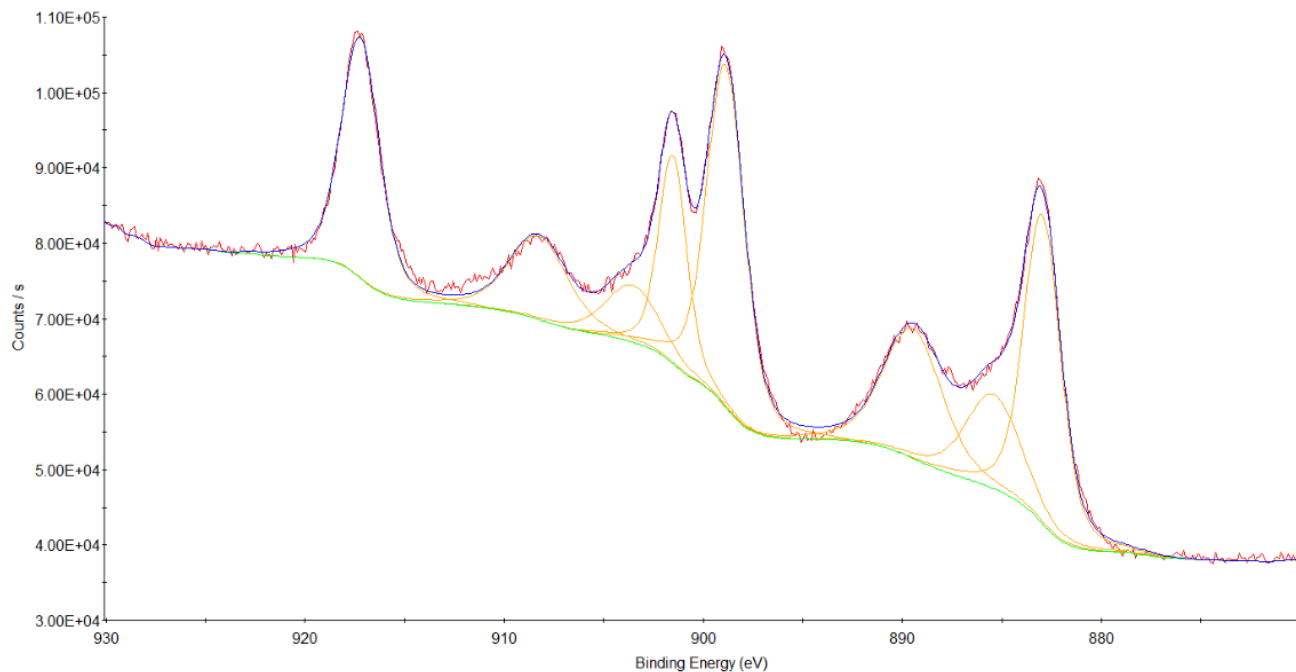


Figure 13. Cerium XPS spectra of 500°C annealed sample exposed to ambient air for 2 weeks. No observable change is noted between the freshly annealed sample (**Figure 11**) and this air exposed sample. Image gathered and analyzed with Thermo Scientific™ Avantage Data System software.

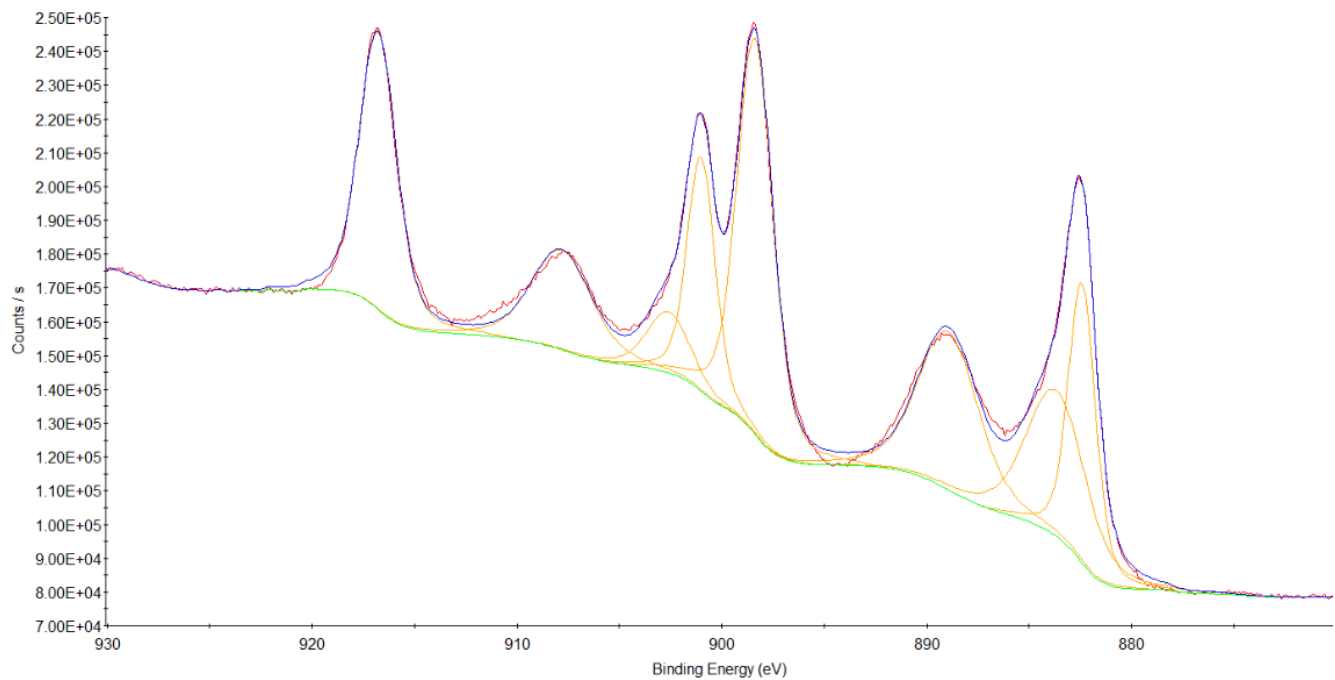


Figure 14. Cerium XPS spectra after UV/Ozone treatment for 20 minutes. Slight reduction of Ce(III) peak is observed in comparison to untreated samples. Image gathered and analyzed with Thermo ScientificTM Avantage Data System software.

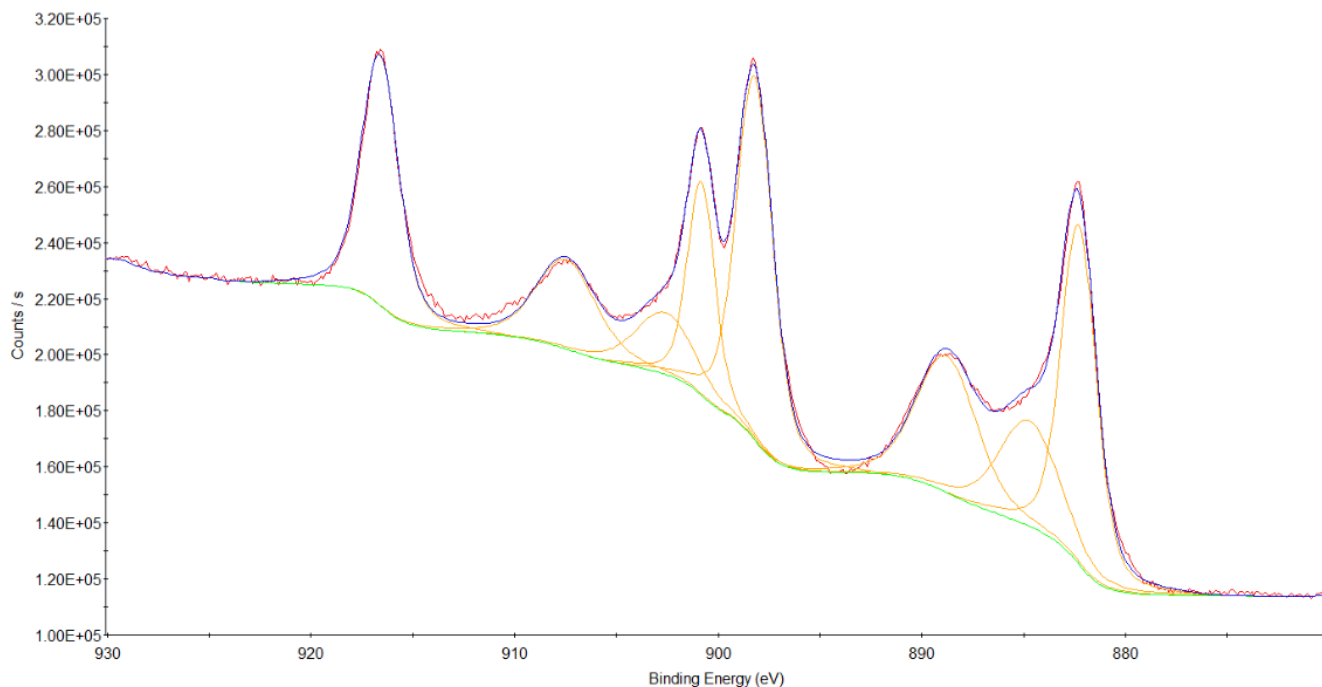


Figure 15. Cerium XPS spectra after Solvent Washing. XPS spectra was taken after 10 seconds of acetone wash, followed by 10 seconds of DI water wash. Identical spectra are observed for increased washing times. Reduction of Ce(III) species is observed. Image gathered and analyzed with Thermo Scientific™ Avantage Data System software.

Reduction of Ce(III) ratio is observed for each surface cleaning method. This includes solvent cleaning. However, this is not the case for Ar^+ sputtering. Sputtering with an ion beam energy of 4000eV produces observable changes on the surface, via an increase the Ce(III) ratio (**Figure 16**). Complete carbon removal was observed after 1 second etching at this higher etching energy.

Sputtering at a much lower energy, 500eV, for 10 seconds produces the same trends seen the other cleaning methods (**Figures 12-15**). A reduction in the Ce(III) ratio (**Figure 17**) was observed by sputtering at this lower energy. Complete removal of surface carbon was observed after 5 seconds of etching. After each case of sputtering, an increase of cerium oxide peaks is observed. This is due to the decrease of surface carbon content, which allows the XPS to further penetrate into the oxide surface.

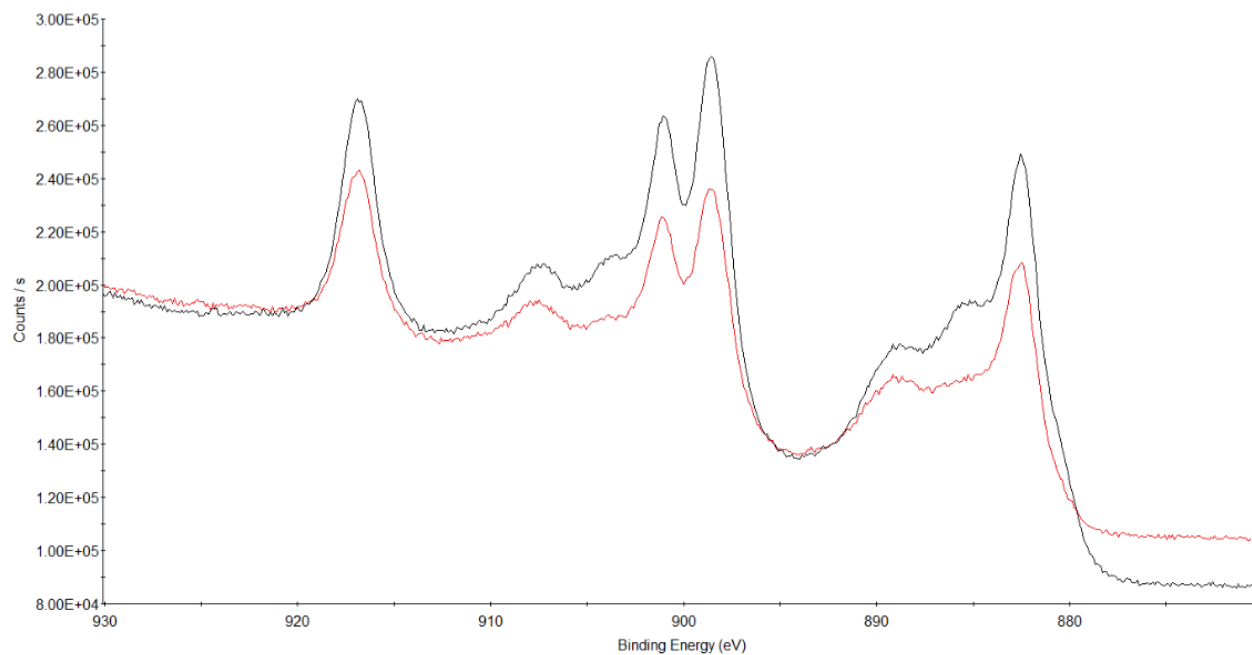


Figure 16. Cerium Oxide spectra comparison after Ar⁺ sputtering at 4000eV. As-received, aged, cerium oxide wafer (**red**) compared to sputtering at 4000eV for 10 seconds (**black**). Image gathered and analyzed with Thermo ScientificTM Avantage Data System software.

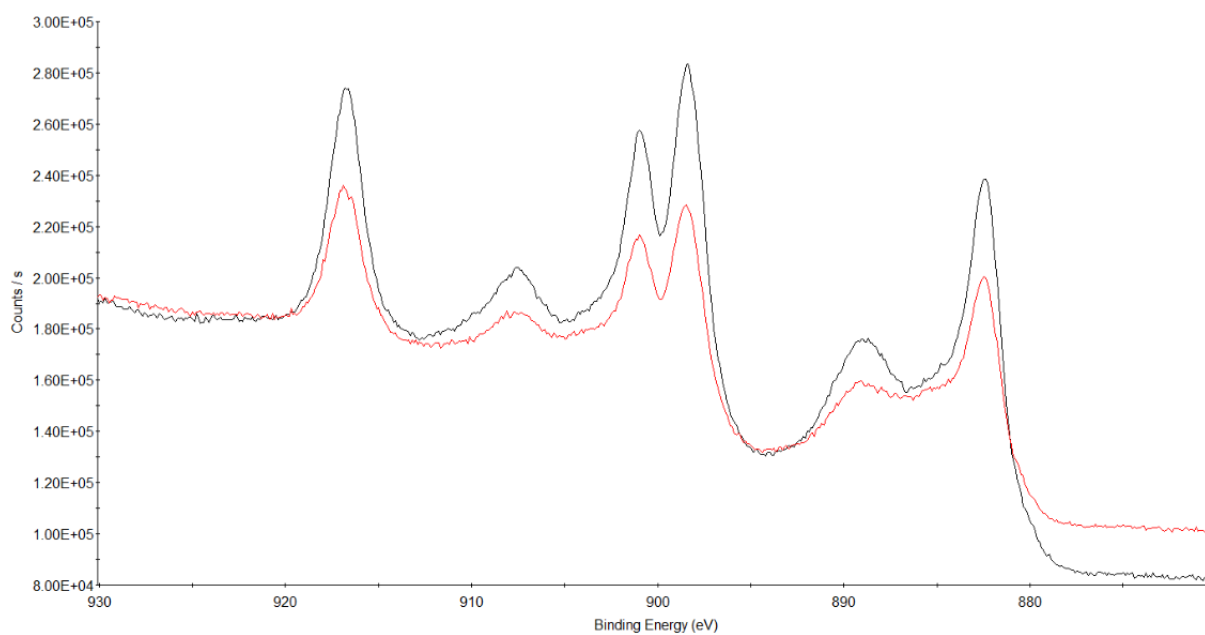


Figure 17. Cerium Oxide spectra comparison after Ar⁺ sputtering at 500eV. As-received, aged, cerium oxide wafer (red) compared to sputtering at 500eV for 10 seconds (black). Image gathered and analyzed with Thermo ScientificTM Avantage Data System software.

4.4 PEAK RATIOS TO QUANTIFY CE⁴⁺:CE³⁺ RATIO

To quickly and precisely quantify the effect of various cleaning methods on the Ce⁴⁺ to Ce³⁺ ratio, a novel technique was used based on observations of trends within each oxidation state of cerium. This technique was implemented due to peak overlap of the Ce⁴⁺ and Ce³⁺ species occurring at 898eV (**Figure 10**), complicating the deconvolution process for species ratio analysis.

The peaks of Ce⁴⁺ were observed to appear in particular ratios between one another; this was also the case for Ce³⁺. Such ratios were calculated via deconvolution of various cerium oxide spectra, as well as from principal component analysis generated Ce³⁺ and Ce⁴⁺ spectra. Since these peaks occur in precise ratios to one another, a correlation factor could be generated to allow easy mathematical manipulation from one integrated peak area to total oxide species integrated area. Therefore, by knowing the peak area of just one peak of each oxide species (Ce⁴⁺ vs Ce³⁺), it can be quickly correlated to a Ce⁴⁺ to Ce³⁺ ratio. An simple relation as set up, equation (2).

$$\begin{array}{l} \text{Total Integration} = (C_f) * (A_n) \\ C_f \longrightarrow \text{Correlation factor of Peak } n \text{ for Total Area} \\ A_n \longrightarrow \text{Area of Peak } n \end{array} \quad (2)$$

The deconvoluted peaks were arbitrarily labeled A through F for Ce⁴⁺ and A through D for Ce³⁺, with A corresponding to the peak with the highest BE, and the last letter corresponding to the peak with the lowest BE. Correlation factors (C_f), with their corresponding peak, are

listed in Table 3. The highlighted peaks were used to calculate total species peak areas for Ce^{3+} and Ce^{4+} respectively. These peaks were chosen due to their consistency and isolation from nearby peaks. These correlation values were then directly related to total oxide species area, from which Ce(IV) to Ce(III) ratios were calculated. The results are shown in Table 4.

Table 3. Relative Composition of Single Peaks and Correlation Factors

Cerium (III)			Cerium (IV)		
Peak	Relative %	C_f	Peak	Relative %	C_f
A	22.25	4.49	A	11.4	8.77
B	20.13	4.97	B	6.53	15.31
C	34.19	2.92	C	21.41	4.67
D	23.43	4.27	D	19.01	5.26
			E	9.34	10.71
			F	32.31	3.1

Table 4. Ce⁴⁺ and Ce³⁺ Peak Ratios After Cleaning and Aging

Cleaning Method	Ce(IV):Ce(III) Ratio
Untreated/Aged	2.9 : 1
500°C Anneal	5.5 : 1
500°C Anneal_2 Week Air Exposure	5.3 : 1
UV/Ozone	6.4 : 1
Ar+ Sputtering	5.9 : 1
Solvent Washing	4.5 : 1

An increase of the Ce⁴⁺ to Ce³⁺ ratio is observed after each cleaning method. This is as expected, since the bulk of the Ce³⁺ would reside on the surface of the cerium oxide thin film. Further experimentation, such as ARXPS, could be performed to confirm this. As the contamination layer was removed by various cleaning methods, the XPS was able to access more

of the bulk cerium oxide, virtually increasing the Ce^{4+} to Ce^{3+} ratio. However, complete recovery of this ratio was not observed in the cleaned samples that were then re-contaminated by aging in air. This suggests that there is an alteration in the surface chemistry of the substrate through each cleaning method. This result does not discount the hydrophilic nature of cleaned REOs, however surface defects via cleaning must be taken into consideration when selecting contamination cleaning methods.

5.0 CONCLUSIONS AND FUTURE DIRECTIONS

In summary, this experimental data strongly support that REOs are intrinsically hydrophilic and become hydrophobic due to the adsorption of airborne carbon-based contaminants on their surfaces. This suggests that the performance of REO-based hydrophobic coatings will depend on the presence of hydrocarbons in the environment and may be negatively impacted if the adsorbed hydrocarbons are removed by thermal or oxidative (*e.g.*, UV/O₃) processes, ion beam etching, or solvent interaction.

Further analysis on samples would involve use of SIMS or TD-MS for precise molecular composition of the surfaces. This would provide information on kinetics and the adsorptive and desorptive properties of molecules on differently prepared samples (eg. Thermal annealing vs. sputtering). Additionally, low-energy ion scattering (LEIS) could be coupled with Ar⁺ ion beam etching. LEIS provides data similar to XPS; however, it would detect the atoms within the first few molecular layers of the sample. By coupling LEIS with Ar⁺ sputtering, precise layer thicknesses of carbon adsorption could be calculated, as well as the precise surface chemistry of the CeO₂. Another method to determine surface chemistry of the CeO₂ wafer would be to couple Ar⁺ sputtering with angle resolved XPS (ARXPS). Angle resolved provides more sensitive data from the surface of the sample by tilting the sample at a particular angle (the XPS beam therefore interacts more with the surface rather than the bulk).

Further experimentation would also involve analyzing other metals/metal oxides and determining correlations between sample lattice orientation or electronic structure of the samples and the carbon contamination identity and adsorption rate or strength. The information determined from such studies will contribute to the efforts of understanding contamination and control on surfaces and progress the field of hydrophobic surfaces. By developing a knowledge base in this matter, in which the interfacial chemistry of surfaces influences its performance after particular storage conditions, it may be possible to optimize interface properties. This may allow for tunable surfaces to control adsorption and desorption under select conditions.

REFERENCES

1. W.R. Tyson, W.A. Miller Surf. Sci., 62 (1977), p. 267
2. J.M. Blakely, Introduction to the Properties of Crystal Surfaces (Pergamon, 1973)
3. Castle, J. E.(2008) 'The Composition of Metal Surfaces After Atmospheric Exposure: An Historical Perspective', The Journal of Adhesion, 84: 4, 368 — 388
4. Lobato, Emilio Marcus de Castro (2004). *Determination of Surface Free Energies and Aspect Ratio of Talc*. M. S. thesis. Virginia Tech. USA
5. Kohli, Rajiv, and K. L. Mittal. "Wettability Techniques to Monitor Cleanliness of Surfaces." *Developments in Surface Contamination and Cleaning*. Norwich, NY, U.S.A.: W. Andrew Pub., 2008. 693-723. Print.
6. Bolger, J. C. and Michaels, A. S., Interface Conversion for Polymer Coatings,P. Weiss and G Cleever (Eds.) (Elsevier, New York, 1968), pp. 3–60.
7. Sparnaay, M. J., Science and Technology of Surface Coating , B. N. Chapman and J. C. Anderson (Eds.) (Academic Press, London-New York, 1974). ch. 1
8. Young T 1805 *Phil. Trans. R. Soc. Lond.* 95, 65-87
9. Kohli, Rajiv, and K. L. Mittal. " Airborne Molecular Contamination: Contamination on Substrates and the Environment in Semiconductors and Other Industries." *Developments in Surface Contamination and Cleaning*. Norwich, NY, U.S.A.: W. Andrew Pub., 2008. 329-474. Print.
10. S. B. Zhu, "Modeling of Airborne Molecular Contamination," Proc. of Annual Technical Meeting of the IEST, 391 (1998)
11. Akihiro, K., *et. al.*" Adsorption properties of SO₂ gas to the HDD disk substrate in a clean room environment." Aerosol Research. Vol. 20, 2005, No. 2 P 153-159
12. Kohli, Rajiv, and K. L. Mittal. "Relevance of Particle Transport in Surface Deposition and Cleaning." *Developments in Surface Contamination and Cleaning*. Norwich, NY, U.S.A.: W. Andrew Pub., 2008. 267-297. Print.
13. Habuka, H.; Shimada, M.; Okuyama, K. "Adsorption and Desorption Rate of Multicomponent Organic Species on Silicon Wafer Surface." *J. Electrochem. Soc.* 2001 148(7): G365-G369
14. Kohli, Rajiv, and K. L. Mittal. "Surface Analysis Methods for Contaminant Identification." *Developments in Surface Contamination and Cleaning*. Norwich, NY, U.S.A.: W. Andrew Pub., 2008. 585-652. Print.
15. Hayun, S.; Shvareva, T. Y.; Navrotsky, A. *J Am Ceram Soc* 2011, 94, 3992.
16. Gennard, S.; Cora, F.; Catlow, C. R. A. *J Phys Chem B* 1999, 103, 10158.
17. Kozbial, A.; Li, Z. T.; Conaway, C.; McGinley, R.; Dhingra, S.; Vahdat, V.; Zhou, F.; D'Urso
18. Kim, K. H.; Jahan, S. A.; Kabir, E.; Brown, R. J. C. *Environ Int* 2013, 60, 71.
19. Li, Z. T.; Wang, Y. J.; Kozbial, A.; Shenoy, G.; Zhou, F.; McGinley, R.; Ireland, P.; Morganstein, B.; Kunkel, A.; Surwade, S. P.; Li, L.; Liu, H. T. *Nat Mater* 2013, 12, 925.
20. Naydenov, A., R. Stoyanova, and D. Mehandjiev, *J. Mol. Catal. A*, 98:9–14 (1995)
21. K. S. Kim and R. E. Davis, *J. Electron Spectrosc.*, 1, 493 (1972).

22. Kohli, Rajiv, and K. L. Mittal. "Cleaning with Solvents." *Developments in Surface Contamination and Cleaning*. Norwich, NY, U.S.A.: W. Andrew Pub., 2008. 759-871. Print.
23. Li, X. M.; Reinhoudt, D.; Crego-Calama, M. *Chem Soc Rev* 2007, 36, 1529.
24. Azimi, G.; Dhiman, R.; Kwon, H. M.; Paxson, A. T.; Varanasi, K. K. *Nat Mater* 2013, 12, 315.
25. Khan, S; Azimi, G; Yildiz, B; Varanasi K. *Applied Physics Letters* 106, 061601 (2015); doi: 10.1063/1.4907756
26. Li, Z. T.; Wang, Y. J.; Kozbial, A.; Shenoy, G.; Zhou, F.; McGinley, R.; Ireland, P.; Morganstein,